PHYSICAL REVIEW D VOLUME 35, NUMBER 3 1 FEBRUARY 1987

Factorization of helicity amplitudes and angular correlations for electroweak processes

Fredrick Olness and Wu-Ki Tung
Department of Physics, Illinois Institute of Technology, Chicago, Illinois 60616
(Received 10 April 1986)

Reliable information on the gauge coupling between W's and Z's can best be obtained from studying angular correlations of electroweak processes. A simple, general method of directly writing down helicity amplitudes for tree diagrams suitable for studying angular correlations is presented. Emphasis is placed on *factorization* properties of these amplitudes which automatically exhibit the physical energy and angular dependences in explicit form. Illustrative examples, including $e^+e^-\to W^+W^-$, are worked out in detail. Applications to angular-correlation studies are outlined.

I. INTRODUCTION

In the wake of the discovery of the intermediate vector bosons of the electroweak interaction, the focus of high-energy experimental physics is shifting toward the elucidation of the Higgs sector and of the gauge coupling between the vector bosons. Detailed studies of W- and Z-boson physics can, in addition, reveal unexpected features which signify the onset of "new physics" beyond the standard model.[1-3] The most often cited "test" of the gauge coupling of the vector bosons is the measurement of the energy dependence of vector-boson pair production,[4-7] where cancellation between two or more tree diagrams in the theory help prevent the theoretical cross section from violating the unitary bound at high energies. Since *any* viable theory, regardless of details, must respect unitarity, it should be rather obvious that reasonable energy dependence of the production cross section alone does not provide a useful test of a specific theory such as the standard model. In contrast, the angular dependence of the produced particles and the angular correlations of their decay products depend critically on the specific gauge couplings, and hence provide more sensitive tests of the underlying theoretical structure.[4-6]

Motivated by this consideration, we have embarked on a systematic study of helicity amplitudes of electroweak processes using a general formalism particularly suited to analyze angular correlations.[8] The method emphasizes the *factorization* properties of tree diagrams which allow us to reduce the helicity amplitudes to standardized vertices connected by (rotational) "D functions." The factorization simplifies the calculation; but, more importantly, the angular factors (production and decay D functions) and the energy-dependence factors (production and decay vertices) are naturally exhibited in a way suitable for immediate application to angular-correlation studies. Features of any theoretical model can be formulated precisely in terms of the vertex structures. Predictions of the standard model can be succinctly stated in terms of a set of relations between experimentally measurable angular-correlation or asymmetry parameters. Thus, possible deviations from the standard model can be conveniently parametrized for phenomenological studies.

We shall denote by l a light charged lepton and ν_l its associated neutrino. Both particles are taken to have negligible mass compared to other mass scales of the process to be considered. The resulting theory, with definite chiral-symmetry properties, becomes particularly simple when analyzed in the way we propose. The vector-boson masses are fully taken into account in all calculations. Since we are dealing with the electroweak process, only tree diagrams are considered.

This paper, the first in a planned series, presents the basic formalism and several illustrative examples. Detailed applications to W-, Z-, and Higgs-boson physics as well as to QCD and supersymmetry physics will be presented in subsequent studies. This paper, focused on factorization and electroweak processes, is in contrast with several recent papers on the use of helicity amplitudes to calculate high-energy multiparticle QCD processes.[9-11] The latter key on simplifications brought about by the massless vector particle (gluon). The two methods are complementary in many ways, and can be combined in applications to a variety of processes.

In Sec. II (Sec. IV) we present the basic formalism for Feynman diagrams involving an s-channel vector-boson (fermion) pole and work out the illustrative example $e^+e^-\to\mu^+\mu^-$ ($W^+e^-\to W^+e^-$). In Sec. III (Sec. V) we do the same for diagrams with a t-channel vector-boson (fermion) pole and compute their contribution to the process $e\mu\to e\mu$ ($ee\to WW$). In Sec. VI we work out the full amplitudes of $e^+e^-\to W^+W^-$ in the standard model.[12] In Sec. VII we discuss how these results can facilitate the study of angular correlations and the test of the standard model and its extensions. In the concluding section (Sec. VIII) we summarize the distinguishing features of this approach, contrast it with the traditional Dirac-trace method, and briefly comment on the relation to the spinor method of the CALKUL and Tsinghua groups[9,10]

II. s-CHANNEL VECTOR-BOSON POLE

Consider the simple process

$$ll'\to V^*\to pp' \tag{2.1}$$

depicted in Fig. 1, where (l,l') is a lepton-antilepton pair

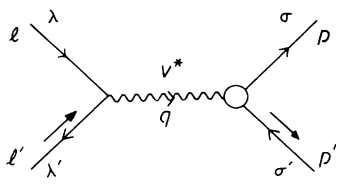

FIG. 1. s-channel vector-boson pole diagram.

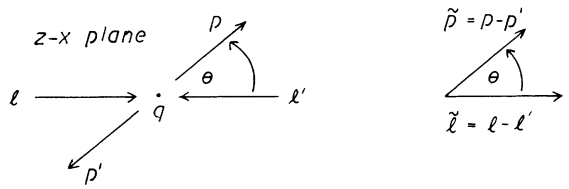

FIG. 2. s-channel center-of-mass kinematics and rotation $R_2(\theta)$, Eq. (2.6).

(not necessarily carrying the same weak charge), V^* a virtual vector boson, and p,p' a pair of arbitrary particles of spin s,s', respectively. The helicities of the particles are denoted by $(\lambda,\lambda',\sigma,\sigma')$ as indicated in the figure. The helicity amplitudes for this process can be written as

$$f^{\sigma\sigma'}_{\lambda\lambda'} = -J^{\sigma\sigma'}_{\mu}(p,p')^* \frac{g^{\mu}{}_{\nu}+q^{\mu}q_{\nu}/M_V{}^2}{q^2+M_V{}^2} j^{\nu}_{\lambda\lambda'}(l,l') \ , \tag{2.2}$$

where $j^{\nu}_{\lambda\lambda'}$ is the lepton vertex function

$$\begin{aligned} j^{\nu}_{\lambda\lambda'}(l,l') &= \langle 0 \mid j^{\nu}(0) \mid l,\lambda;l',\lambda' \rangle \\ &= \bar{v}_{\lambda'}(l')\gamma^{\nu}\left[g_L \frac{(1-\gamma^5)}{2} + g_R \frac{(1+\gamma^5)}{2}\right] u_{\lambda}(l) \end{aligned} \tag{2.3}$$

and $J^{\sigma\sigma'}_{\mu}$ represents the general vertex function

$$\begin{aligned} J^{\sigma\sigma'}_{\mu}(p,p')^* &= [J^{\mu}_{\sigma\sigma'}(p,p')]^* \\ &= \langle p,\sigma;p',\sigma' \mid J^{\dagger}_{\mu}(0) \mid 0 \rangle \ . \end{aligned} \tag{2.4}$$

The latter will reduce to an expression similar to Eq. (2.3) if the final state also consists of a lepton-antilepton pair.

It is well known that the second-rank tensor in the numerator of the propagator corresponds to a spin-projection operator of the virtual vector boson. Our approach consists of making this fact manifest and of rewriting the propagator in a factorized form.[13] Thus, we observe

$$g^{\mu}{}_{\nu} = q^{\mu}q_{\nu}/q^2 + e^{k}_{m}(q)^{\mu} e^{m}_{k}(q)^*_{\nu} \ , \tag{2.5}$$

where $\{e^{k}_{m}(q),\ m=1,0,-1\}$ are helicity polarization vectors of the virtual vector boson defined with respect to an arbitrary reference (spacelike) vector k. (See Appendix A for details.)

For the process of Eq. (2.1), two distinct reference momenta are relevant: $\tilde{l}=l-l'$, the relative momentum of the initial state; and $\tilde{p}=p-p'$, that of the final state. The two sets of polarization vectors $\{e^{l}_{m}(q)\}$ and $\{e^{p}_{m}(q)\}$ are related by a simple rotation in the common center-of-mass frame. If we pick the z axis to be along the initial-state relative momentum $\tilde{l}$ and the x-z plane to coincide with the scattering plane (Fig. 2), then

$$\begin{aligned} e^{p}_{m}(q)^{\mu} &= \Lambda[R_2(\theta)]^{\mu}{}_{\nu} e^{l}_{m}(q)^{\nu} \\ &= e^{l}_{n}(q)^{\mu} d^{1}(\theta)^{n}{}_{m} \ , \end{aligned} \tag{2.6}$$

where θ is the scattering angle, $\Lambda[R_2]$ is the (4×4) Lorentz transformation matrix for the rotation $R_2(\theta)$, and $d^{1}(\theta)$ is the standard rotational matrix (around the y axis) for angular momentum one [cf. Appendix A]. Equation (2.6) implies,

$$e^{m}_{p}(q)^*_{\nu} = d^{1\dagger}(\theta)^{m}{}_{n} e^{n}_{l}(q)^*_{\nu} = d^{1}(-\theta)^{m}{}_{n} e^{n}_{l}(q)^*_{\nu} \ . \tag{2.7}$$

Substituting into Eq. (2.5), with k set equal to $\tilde{p}$, we obtain

$$g^{\mu}{}_{\nu} = q^{\mu}q_{\nu}/q^2 + e^{p}_{m}(q)^{\mu} d^{1}(-\theta)^{m}{}_{n} e^{n}_{l}(q)^*_{\nu} \ . \tag{2.8}$$

We are now ready to exhibit the factorized structure of the helicity amplitudes. Making use of Eqs. (2.5) and (2.8) we can rewrite Eq. (2.2) as

$$\begin{aligned} f^{\sigma\sigma'}_{\lambda\lambda'}(s,\theta) &= J^{\sigma\sigma'}_{m}(s)^* \frac{d^{1}(-\theta)^{m}{}_{n}}{s-M_V{}^2} j^{n}_{\lambda\lambda'}(s) \\ &\quad + J^{\sigma\sigma'}_{q}(s)^* \frac{1}{M_V{}^2} j^{q}_{\lambda\lambda'}(s) \ , \end{aligned} \tag{2.9}$$

where

$$\begin{aligned} j^{n}_{\lambda\lambda'}(s) &= e^{n}_{l}(q)^*_{\nu} j^{\nu}_{\lambda\lambda'}(l,l') \ , \\ J^{\sigma\sigma'}_{m}(s)^* &= J^{\sigma\sigma'}_{\mu}(p,p')^* e^{p}_{m}(q)^{\mu} \ , \end{aligned} \tag{2.10}$$

and $j^{q}_{\lambda\lambda'}(s)$ and $J^{\sigma\sigma}_{q}(s)^*$ are analogous expressions with the polarization vectors above replaced by the unit vector $e^{\mu}_{q}=q^{\mu}/\sqrt{s}$ where $-q^2=s$.

We note several important features of Eqs. (2.9) and (2.10).

(i) The two terms on the right-hand side of Eq. (2.9) are *factorized* in that the vertex factor $j_{\lambda\lambda'}(s)$ $[J^{\sigma\sigma'}(s)]$ only depends on the initial- [final-] state parameters and the common energy variable s. The propagator factor explicitly exhibits the effect of the rotation which relates the final configuration to the initial configuration. The entire dependence on the scattering angle resides in the d-function factor. The factorization of the general scattering amplitude into the basic building blocks ($j_{\lambda\lambda}$ and d functions) is the key to this approach (cf. Fig. 3). The d

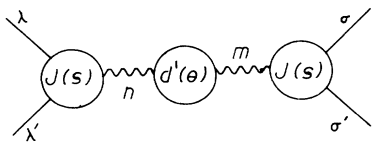

FIG. 3. Diagrammatic representation of the factorized amplitude, Eq. (2.9).

functions are specified in Appendix A and the fundamental vertex functions are derived in Appendix B.

(ii) The vertex factors $j^n_{\lambda\lambda'}(s)$ $[J_m^{\sigma\sigma'}(s)]$ have the natural physical interpretation as helicity amplitudes which represent the emission [absorption] of a vector boson of polarization vector e_ν^{m*} $[e_m^\mu]$. Likewise, $j^q_{\lambda\lambda'}(s)$ $[J_q^{\sigma\sigma'}(s)]$ represents the helicity amplitudes of emission [absorption] of a "scalar" boson (with respect to 3-rotations) with polarization four-vector e_q^μ. We shall refer to these quantities as *helicity vertex amplitudes.*

(iii) Furthermore, $j^n_{\lambda\lambda'}(s)$ and $J_m^{\sigma\sigma'}(s)$ are Lorentz scalars, and hence are independent of the choice of coordinate axes; in particular, they can be conveniently calculated in the center-of-mass frame with all momenta aligned along the z axis (see Fig. 4). *Angular-momentum conservation* requires that

$$\begin{aligned} j^n_{\lambda\lambda'}(s)&=\delta^n_{\lambda-\lambda'}j_{\lambda\lambda'}(s)\ , \\ j^q_{\lambda\lambda'}(s)&=\delta^\lambda_{-\lambda'}j^q_\lambda(s)\ , \end{aligned} \tag{2.11}$$

which defines the quantities on the right-hand sides, together with identical constraints on $J^{\sigma\sigma'}(s)$.

(iv) If the vector boson is coupled to a *conserved current,* then gauge invariance requires that the scalar vertex amplitudes vanish:

$$j^q_{\lambda\lambda'}=0=J_q^{\sigma\sigma'} \text{ for all } \lambda,\ \lambda',\ \sigma,\ \sigma'\ . \tag{2.12}$$

This means, in all practical cases, that the scalar term on the right-hand side of Eq. (2.9) does not contribute to the scattering amplitude.

(v) The vertex amplitude $j_{\lambda\lambda'}(s)$ and $J^q_\lambda(s)$ for a general vector—axial-vector coupling are evaluated in Appendix B. In the limit $m_l=m_{l'}=0$, we have, in addition to (2.11) and (2.12),

$$\begin{aligned} j_{R\bar{R}}(s)&=0=j_{L\bar{L}}(s)\ , \\ j_{L\bar{R}}(s)&=g_L\sqrt{2s}\ , \\ j_{R\bar{L}}(s)&=-g_R\sqrt{2s}\ , \end{aligned} \tag{2.13}$$

where the helicity labels for the leptons take values L,R for left and right handed, respectively. These extremely simple results reflect the well-known fact that vector and axial-vector couplings to fermions are *chirality conserving.* (The helicity and chirality quantum numbers coincide for zero-mass leptons; they are opposite for antileptons.) If the coupling to the vector boson is purely left handed ($g_R=0$) [right handed ($g_L=0$)], then only *one* out of the eight vertex functions, $j_{L\bar{R}}$ $[j_{R\bar{L}}]$, is nonzero.

(vi) If the lepton masses are not set to zero, then the chirality-changing vertex amplitudes $j_{L\bar{L}}$ and $j_{R\bar{R}}$ will be proportional to m_l, and the chirality-conserving vertex amplitudes $j_{L\bar{R}}$ and $j_{R\bar{L}}$ will acquire order-$(m_l{}^2/s)$ correction terms [cf. Eq. (2.13)]. Thus, the helicity vertex amplitudes are, in general, naturally segregated in order of magnitudes according to some appropriate energy scale.

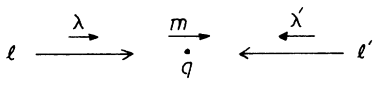

FIG. 4. Kinematics, including angular-momentum components, for the vertex amplitudes, Eqs. (2.10) and (2.11).

We now apply this method to the elementary process

$$e^-(l,\lambda)+e^+(l',\lambda')\to\gamma^*\to\mu^-(p,\sigma)+\mu^+(p',\sigma')\ . \tag{2.14}$$

For the electromagnetic interaction, $g_L=g_R=e$, and the helicity vertex amplitudes are given by Eq. (2.13) for both initial and final states (cf. also Appendix B). The longitudinal and scalar polarizations of γ^* do not couple at all, and hence we obtain zero amplitudes if $\sigma=\sigma'$ or $\lambda=\lambda'$:

$$f^{\sigma\sigma}_{\lambda\lambda'}=0=f^{\sigma\sigma'}_{\lambda\lambda} \quad (\lambda,\lambda',\sigma,\sigma'=R,L)\ . \tag{2.15}$$

The nonvanishing amplitudes are given by the simple expressions

$$\begin{aligned} f^{L\bar{R}}_{L\bar{R}}&=2e^2d^1(-\theta)^{-1}{}_{-1}=e^2(1+\cos\theta) \\ &=2e^2d^1(-\theta)^1{}_1=f^{R\bar{L}}_{R\bar{L}}\ , \end{aligned} \tag{2.16}$$

$$\begin{aligned} f^{L\bar{R}}_{R\bar{L}}&=-2e^2d^1(-\theta)^{-1}{}_1=-e^2(1-\cos\theta) \\ &=-2e^2d^1(-\theta)^1{}_{-1}=f^{R\bar{L}}_{L\bar{R}}\ . \end{aligned} \tag{2.17}$$

Hence, the unpolarized cross section is

$$\frac{d\sigma}{d\Omega}=\frac{1}{64\pi^2s}\frac{1}{4}\Sigma^{\sigma\sigma'}_{\lambda\lambda'}|f^{\sigma\sigma'}_{\lambda\lambda'}|^2=\frac{\alpha^2}{4s}(1+\cos^2\theta)\ , \tag{2.18}$$

a familiar result. The advantages of the current approach (over the Dirac-trace method, say) are that the full information on the polarizations is exhibited in the intermediate steps [Eqs. (2.15)—(2.17)] and that the physics behind these results [i.e., origin of the θ dependence in the $d^1(\theta)$ functions and the energy dependence in the vertex amplitudes] are apparent throughout.

These points are even more clearly seen in the process

$$e+\bar{\nu}_e\to W^-\to\mu+\bar{\nu}_\mu\ . \tag{2.19}$$

With $g_L=g/\sqrt{2}$ and $g_R=0$, our rules immediately yield

$$\begin{aligned} f^{L\bar{R}}_{L\bar{R}}(s,\theta)&=\frac{g^2s}{s-{M_W}^2}d^1(\theta)^{-1}{}_{-1} \\ &=\frac{g^2s}{s-{M_W}^2}\cos^2\frac{\theta}{2}\ , \\ f^{\sigma\bar{\sigma}}_{\lambda\bar{\lambda}}(s,\theta)&=0 \quad \text{otherwise}\ . \end{aligned} \tag{2.20}$$

The full simplicity and physical content of this process is displayed all at once in Eq. (2.20).

III. t-CHANNEL VECTOR-BOSON POLE

We now consider the t-channel diagram, Fig. 5, for scattering of two fermions. The scattering amplitude can be written [cf. Eq. (2.2)] as

$$f^{\sigma\sigma'}_{\lambda\lambda'}=-J^{\sigma'*}_{\lambda'\mu}(l',p')\frac{g^\mu{}_\nu+q^\mu q_\nu/{M_V}^2}{q^2+{M_V}^2}J^{\sigma\nu}_\lambda(l,p)\ , \tag{3.1}$$

where

$$J^{\sigma\nu}_\lambda(l,p)=\langle p,\sigma\,|\,J^\nu(0)\,|\,l,\lambda\rangle\ . \tag{3.2}$$

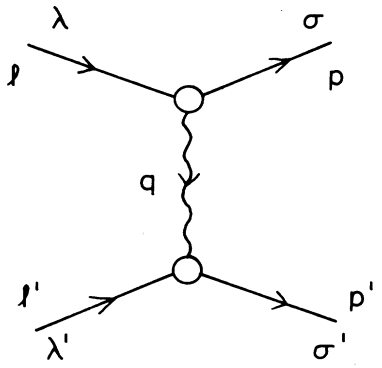

FIG. 5. t-channel vector-boson pole diagram.

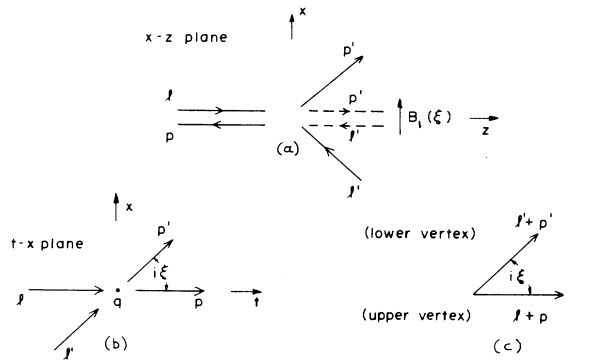

FIG. 6. Brick-wall (Breit) frame kinematics, and Lorentz "rotation" (boost) $B_1(\xi)$, Eq. (3.6): (a), the x-z plane; (b) and (c), the t-x plane.

In order to take advantage of the factorized vertex amplitudes, we need to decompose the vector-boson propagator as before. Toward that goal, we write again

$$g^{\mu}{}_{\nu}=e_q^{\mu}e_{\nu}^{q}+e_m(q)^{\mu}e^{m}(q)_{\nu}^{*}$$
$$=e_q^{\mu}e_{\nu}^{q}+e'_m(q)^{\mu}e'^{m}(q)_{\nu}^{*}\ , \tag{3.3}$$

where the three "vector" polarization vectors $(e_m, m=1,0,-1)$ must be defined with respect to some reference momentum: the unprimed ones (first line) to $l+p$, say, and the primed ones to $l'+p'$. The primed system is related to the unprimed system by an SO(2,1) transformation which leaves q^{μ} invariant (i.e., an element of the little group of q^{μ}).

This relation is most easily seen in the brick-wall (BW) frame defined by

$$q^{\mu}:\ (0,0,0,\sqrt{-t}\,)\ ,$$
$$l^{\mu}:\ (\sqrt{-t}\,,0,0,\sqrt{-t}\,)/2\ , \tag{3.4}$$
$$p^{\mu}:\ (\sqrt{-t}\,,0,0,-\sqrt{-t}\,)/2\ .$$

If the scattering plane is chosen to be the x-z plane, then the configuration of the vectors (l'^{μ},p'^{μ}) are related to that of (p^{μ},l^{μ}) by a boost along the x axis (note that $l-p=q=p'-l'$, cf. Fig. 6)

$$l'^{\mu}:\ (\cosh\xi,\sinh\xi,0,-1)\sqrt{-t}\,/2\ ,$$
$$p'^{\mu}:\ (\cosh\xi,\sinh\xi,0,1)\sqrt{-t}\,/2\ , \tag{3.5}$$

where the hyperbolic angle ξ is related to the velocity of the boost by $\tanh\xi=v/c$. This boost, $B_1(\xi)$, is an element of the little group of q^{μ} (Refs. 13 and 14). Denoting the "spin-1" representation matrix of the SO(2,1) transformation by $\tilde{d}^{\,1}(\xi)$ (Appendix A), we obtain

$$e'_m(q)^{\mu}=\Lambda[B_1(\xi)]^{\mu}{}_{\nu}e_m(q)^{\nu}=e_n(q)^{\mu}\tilde{d}^{\,1}(\xi)^{n}{}_{m} \tag{3.6}$$

and

$$e'^{m}(q)_{\nu}^{*}=\tilde{d}^{\,1}(\xi)^{m}{}_{n}e^{n}(q)_{\nu}^{*}\ . \tag{3.7}$$

Substituting Eq. (3.7) in Eqs. (3.1) and (3.3) yields the desired result (cf. Fig. 7):

$$f^{\sigma\sigma'}_{\lambda\lambda'}(t,\xi)=J^{\sigma'}_{\lambda'm}(t)^{*}\frac{\tilde{d}^{\,1}(\xi)^{m}{}_{n}}{t-M_V{}^2}J^{\sigma n}_{\lambda}(t)\ , \tag{3.8}$$

where $t=-q^2$ and the invariant vertex amplitudes are

$$J^{\sigma n}_{\lambda}(t)=e^{n}(q)^{*}_{\nu}J^{\sigma\nu}_{\lambda}(l,p)\ . \tag{3.9}$$

We have left out the scalar vertex contribution to Eq. (3.8) since it vanishes for conserved currents or for massless fermions. The vertex amplitudes $J^{\sigma n}_{\lambda}$ are of the standard form given in Appendix B.

Let us apply this method to

$$e^{-}+\mu^{+}\to e^{-}+\mu^{+} \tag{3.10}$$

by γ^{*} exchange. In the BW frame, the two fermions at each vertex move in opposite directions. Hence, according to the rules of Appendix B, only transverse polarizations of the virtual-photon contribute. The nonvanishing vertex amplitudes have the common magnitude

$$2\sqrt{-l\cdot p}=\sqrt{-2t}\ . \tag{3.11}$$

We obtain

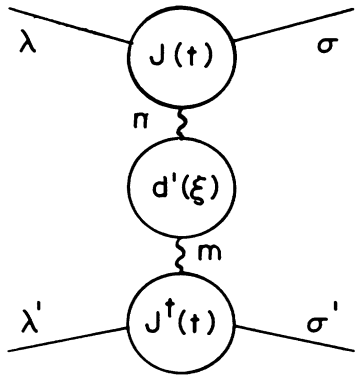

FIG. 7. t-channel factorization of helicity amplitudes, Eq. (3.8).

$$f_{RR}^{RR}=f_{LL}^{LL}=-2e^2\tilde{d}^{\,1}(\xi)^{+}{}_{+}=-e^2(1+\cosh\xi)\ ,$$
$$f_{RL}^{RL}=f_{LR}^{LR}=2e^2\tilde{d}^{\,1}(\xi)^{+}{}_{-}=e^2(1-\cosh\xi)\ . \tag{3.12}$$

Hence the differential cross section is

$$\frac{d\sigma}{d\Omega}=\frac{\alpha^2}{4s}(1+\cosh^2\xi)\ . \tag{3.13}$$

We can express $\cosh\xi$ in terms of s-channel variable by noting that

$$\cosh\xi=(l+p)(l'+p')/t=-2\frac{s}{t}-1=\frac{3+\cos\theta}{1-\cos\theta}\ , \tag{3.14}$$

where θ is the c.m. scattering angle. Substituting Eq. (3.14) in Eq. (3.13), one recovers the well-known result

$$\frac{d\sigma}{d\Omega}=\frac{\alpha^2}{2s}\frac{1+\cos^4\theta/2}{\sin^4\theta/2}\ . \tag{3.15}$$

It is also of interest to note that the results above, along with those of Sec. II, can be applied to Bhabha scattering, $e^-+e^+\to e^-+e^+$, for which both the t-channel and the s-channel amplitudes contribute. We obtain

$$f_{RL}^{LR}=f_{LR}^{RL}=-e^2(1-\cos\theta)\ ,$$
$$f_{RL}^{RL}=f_{LR}^{LR}=e^2[(1+\cos\theta)+(1-\cosh\xi)]$$
$$=-e^2\frac{(1+\cos\theta)^2}{1-\cos\theta}\ , \tag{3.16}$$
$$f_{RR}^{RR}=f_{LL}^{LL}=-e^2(1+\cosh\xi)=-e^2\frac{4}{1-\cos\theta}\ .$$

Thus, only the two amplitudes in the middle line involve s-t-channel interference. The other amplitudes consist of either pure s-channel exchange, or t-channel exchange. The unpolarized cross section is

$$\frac{d\sigma}{d\Omega}=\frac{\alpha^2}{8s}\left[(1-\cos\theta)^2+\frac{(1+\cos\theta)^4}{(1-\cos\theta)^2}+\frac{16}{(1-\cos\theta)^2}\right]$$
$$=\frac{\alpha^2}{2s}\frac{1}{\sin^4\theta/2}\left[1+\sin^8\frac{\theta}{2}+\cos^8\frac{\theta}{2}\right]\ . \tag{3.17}$$

The last result is the ultrarelativistic limit of the Bhabha cross section.

The helicity-amplitude structure of the analogous weak processes, $\nu_\mu+e^-\to\mu^-+\nu_e$, $\nu_e+e^-\to\nu_e+e^-$, . . . , are even simpler than the above example; each process has only one nonvanishing amplitude. The relevant polarizations of the fermions and the associated angular and energy dependences can all be inferred by simple physical arguments are presented previously (see the last paragraph of Sec. II).

IV. s-CHANNEL FERMION POLE

The above approach can be applied to diagrams with a fermion pole provided a suitable factorization of the fermion propagator can be formulated. Let us consider the process depicted in Fig. 8. The amplitude can be written as

$$f_{\lambda m}^{\lambda' m'}=\bar{u}^{\,\lambda'}(l')e^{m'}(q')^{*}_{\mu}\Gamma'^{\mu}\frac{-\not p}{s}\Gamma_\nu e_m(q)^\nu u_\lambda(l)\ , \tag{4.1}$$

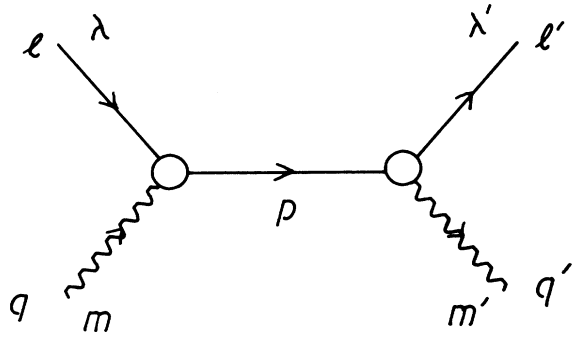

FIG. 8. s-channel fermion pole diagram.

where Γ and Γ' denote the unspecified coupling of the vector bosons to the fermions at the two vertices, respectively. In order to factorize this amplitude into independent vertices, we need to recast the numerator of the propagator $\not p$ in the form of a product of Dirac spinors, and the factors must only refer to either the initial-state or final-state variables in the manner of Eq. (2.8) for the vector boson.

Consider the incoming channel first. Let the momenta l^μ and q^μ determine the t-z axes. We can write the momentum p as the sum of two lightlike vectors $p_\pm^\mu$ moving in opposite directions along the z axis:

$$p^\mu=l^\mu+q^\mu\equiv p_+^\mu+p_-^\mu\ ,$$
$$p_+^\mu:\ \frac{p^0+p^3}{2}(1,0,0,+1)\ , \tag{4.2}$$
$$p_-^\mu:\ \frac{p^0-p^3}{2}(1,0,0,-1)\ .$$

It then follows that

$$-\not p=-\not p_+-\not p_-=u_\lambda(p_+)\bar{u}^{\,\lambda}(p_+)$$
$$+u_\lambda(p_-)\bar{u}^{\,\lambda}(p_-)\ , \tag{4.3}$$

where $u_\lambda(p_\pm)$ are on-shell Dirac spinors representing lightlike particles moving along the z axis with momenta $p_\pm$, respectively. The decomposition in Eq. (4.3) is the fermion equivalent of Eq. (2.5) for the boson propagator. When l^μ and q^μ are both lightlike, and move in opposite directions (say right moving and left moving, respectively) then $p_+=l$ and $p_-=q$. This will not be true when the vector boson is massive.

As in the previous case, the above definition of $u_\lambda(p_\pm)$ depends, in addition to the vector p^μ, on a reference momentum (say, $l^\mu-q^\mu$) which together with p determines the t-z axes. When this fact needs to be made explicit, we add an extra label i (for "initial") to the spinors. It should be obvious that an equivalent decomposition with respect to the final channel also holds, i.e.,

$$-\not p=\sum_{\lambda,\tau}u_\lambda^i(\tau)\bar{u}_i^{\,\lambda}(\tau)=\sum_{\lambda,\tau}u_\lambda^f(\tau)\bar{u}_f^{\,\lambda}(\tau)\ , \tag{4.4}$$

where $\tau=\pm$, and for simplicity we write $u_\lambda(\pm)$ for

$u_\lambda(p_\pm)$. The spinors $\{u^f_\lambda(\tau)\}$ are related to $\{u^i_\lambda(\tau)\}$ by a rotation in the common c.m. frame. In Appendix A, we determine the relation to be

$$u^f_\lambda(\tau)\equiv R_2(\theta)u^i_\lambda(\tau)=u^i_\lambda(\tau')d^{1/2}(\theta)^{\tau'}{}_\tau \tag{4.5}$$

[cf. Eq. (A21)], where θ is the scattering angle. Note that the helicity index remains invariant as expected for massless particle states, while the τ index (i.e., direction of motion) mixes under the rotation. We obtain, therefore,

$$-\not{p}=u^f_\lambda(\tau')d^{1/2}(-\theta)^{\tau'}{}_\tau\bar{u}^\lambda{}_i(\tau)\ , \tag{4.6}$$

where all repeated indices are summed.

The helicity scattering amplitude, Eq. (4.1), can now be written as

$$f^{\lambda'm'}_{\lambda m}(s,\theta)=\frac{1}{s}J^{\lambda'm'}_{\sigma;\tau'}(s)^*d^{1/2}(-\theta)^{\tau'}{}_\tau J^{\sigma;\tau}_{\lambda m}(s)\ , \tag{4.7}$$

where

$$J^{\sigma;\tau}_{\lambda m}(s)=\bar{u}^\sigma(p_\tau)\Gamma_\nu e_m(q)^\nu u_\lambda(l)\ . \tag{4.8}$$

Equation (4.7) is the desired form for the amplitude which explicitly displays the dependence on s, θ, (λ,m), and (λ',m') in factorized form, and the vertex amplitudes, Eq. (4.8), are of the standard form formulated in Appendix B. The index τ on the vertex amplitude refers to the τ index of $u(p_\tau)$ on the right-hand side of the equation. This index has been suppressed in the preceding sections (and in Appendix B) because, for external fermion lines, the p in $u(p)$ is fixed. Here, due to the decomposition of the fermion propagator, both $p_\pm$ enter [Eqs. (4.4)—(4.6)]. We must make (τ,τ') explicit in Eq. (4.7) since they have to be summed over. In practice, for a given vector-boson helicity (m), only one of the vertex amplitudes $(\tau=\pm)$ is nonvanishing. (See Appendix B for detailed rules, and below for a concrete application.)

We now consider a specific example—electron-W^+ scattering through the s-channel ν pole, $e^-+W^+\to\nu^*\to e^-+W^+$. We shall denote the mass of the W boson by M. In the s-channel c.m. frame we have

$$\begin{aligned} &l^\mu:\ \gamma M(\beta,0,0,\beta)\ ,\\ &q^\mu:\ \gamma M(1,0,0,-\beta)\ , \end{aligned} \tag{4.9}$$

where

$$\begin{aligned} &\beta=(s-M^2)/(s+M^2)\ ,\\ &\gamma=(s+M^2)/2M\sqrt{s}\ . \end{aligned} \tag{4.10}$$

The final-state momenta (l',q') are obtained from (l,q), Eq. (4.9), by a rotation through the angle θ—the s-channel scattering angle. In this frame,

$$p^\mu:\ \sqrt{s}\,(1,0,0,0)\ ; \tag{4.11}$$

hence, according to Eq. (4.2),

$$p^\mu_\pm:\ \frac{\sqrt{s}}{2}(1,0,0,\pm1)\ . \tag{4.12}$$

We further note that

$$\begin{aligned} &-2l\cdot q=s-M^2\ ,\\ &-2l\cdot p_+=0\ ,\\ &-2l\cdot p_-=2M\sqrt{s}\,\gamma\beta=s-M^2\ ,\\ &-2q\cdot p_+=s\ . \end{aligned} \tag{4.13}$$

For left-handed coupling of the W boson, the only nonvanishing transverse vertex amplitude is

$$\begin{aligned} J^{L;-}_{L}(s)&=-2\sqrt{-l\cdot p_-}\\ &=-[2(s-M^2)]^{1/2}=J^{L}_{L;-}(s)\ , \end{aligned} \tag{4.14}$$

and the only nonvanishing longitudinal vertex amplitude is

$$\begin{aligned} J^{L;+}_{L0}(s)&=2[(e_q\cdot l)(e_q\cdot p_+)]^{1/2}\\ &=\frac{-[s(s-M^2)]^{1/2}}{M}=J^{L0}_{L;+}(s) \end{aligned} \tag{4.15}$$

[cf. Appendix B]. It follows immediately that all helicity amplitudes involving right-handed leptons vanish. Applying the above results to the formula for the scattering amplitude, Eq. (4.7), we find the only nonvanishing helicity amplitudes to be

$$\begin{aligned} &f^{L}_{L-}(s,\theta)=\cos\frac{\theta}{2}\ ,\\ &f^{L0}_{L-}(s,\theta)=\eta_s\sin\frac{\theta}{2}=-f^{L-}_{L0}(s,\theta)\ ,\\ &f^{L0}_{L0}(s,\theta)=\eta_s{}^2\cos\frac{\theta}{2}\ , \end{aligned} \tag{4.16}$$

where

$$\eta_s=(s/2M^2)^{1/2}\ . \tag{4.17}$$

In order to exhibit the simple structure of these amplitudes, a common factor

$$N=g^2(1-M^2/s) \tag{4.18}$$

has been suppressed in Eq. (4.16). $(g/\sqrt{2}$ is the fermion-boson coupling constant.)

The above results again illustrate clearly a number of important features of this method. In addition to the simple manner by which the amplitudes can be obtained and the obvious physical interpretation of the angular factors, we note that the energy factor η_s represents the ratio of the longitudinal vertex amplitude, Eq. (4.15), to the transverse vertex amplitude, Eq. (4.14); the number of powers of η_s in each helicity amplitude is just given by the number of longitudinal-polarization indices. At high energies, $\eta_s\gg1$, and the longitudinal amplitude f^{L0}_{L0} becomes the dominant one, as is well known.

V. t-CHANNEL FERMION POLE

The last diagram we examine is one with a t-channel fermion pole, such as in Fig. 9. Combining the techniques introduced in Secs. III and IV above, this case can be treated readily. We shall only draw attention to some nontrivial sign changes.

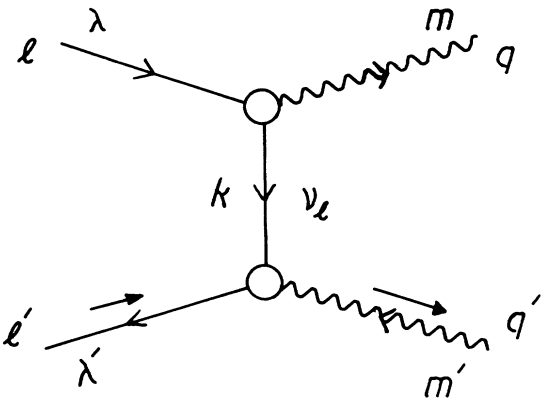

FIG. 9. t-channel fermion pole diagram.

We need to decompose the propagator momentum k^μ into two lightlike four-vectors $k^\mu_\pm$. Since k^μ is spacelike, the decomposition has to be a *difference*, rather than a sum as in Eq. (4.2), if both $k^\mu_\pm$ are to have positive energies; hence,

$$k^\mu = k^\mu_+ - k^\mu_- \ . \tag{5.1}$$

In the BW frame, we have

$$\begin{aligned} &k^\mu\text{: } (0,0,0,\sqrt{-t}\,) \ , \\ &k^\mu_\pm\text{: } (1,0,0,\pm 1)\sqrt{-t}\,/2 \ , \\ &l^\mu\text{: } (1,0,0,1)\gamma_t \ , \\ &q^\mu\text{: } (1,0,0,-\beta_t)\gamma_t \ , \\ &q'^\mu\text{: } (\cosh\xi,\sinh\xi,0,\beta'_t)\gamma'_t \ , \\ &l'^\mu\text{: } (\cosh\xi,\sinh\xi,0,-1)\gamma'_t \ , \end{aligned} \tag{5.2}$$

where

$$\begin{aligned} &\gamma_t = (-t+M^2)/2\sqrt{-t} \ , \\ &\beta_t = (-t-M^2)/(-t+M^2) \ , \end{aligned} \tag{5.3}$$

and with γ'_t and β'_t similarly defined in terms of M'. The vectors for the lower vertex (l'^μ, q'^μ) can be obtained by a Lorentz boost $B_1(\xi)$ from the configuration

$$\begin{aligned} &l'^\mu\text{: } (1,0,0,-1)\gamma'_t \ , \\ &q'^\mu\text{: } (1,0,0,\beta'_t)\gamma'_t \ , \end{aligned} \tag{5.4}$$

which is related to the vectors of the unprimed vertex by a rotation $R_2(\pi)$. We can make use of the results of Appendix A [Eq. (A25)] to obtain

$$-\not{k} = \tau' u'_\sigma(\tau')\tilde{d}^{\,1/2}(\xi)^{\tau'}{}_\tau \bar{u}^{\,\sigma}(\tau) \ , \tag{5.5}$$

where $\tau,\tau' = \pm$, and u (u') represents the spinor quantized with respect to the axis of the unprimed (primed) vertex.

It is now possible to write down the factorized helicity amplitudes

$$f^{mm'}_{\lambda\lambda'}(t,\xi) = \frac{g^2}{2}\frac{1}{t}(\tau')J^{m'}_{\lambda'\sigma}(t)_{\tau'}\tilde{d}^{\,1/2}(\xi)^{\tau'}{}_\tau J^{\sigma m}_\lambda(t)^\tau \ , \tag{5.6}$$

where $g/\sqrt{2}$ is the boson-fermion coupling, and

$$\begin{aligned} &J^{\sigma m}_\lambda(t)^\tau = \bar{u}^{\,\sigma}(k_\tau)\Gamma e^m(q)^* u_\lambda(l) \ , \\ &J^{m'}_{\lambda'\sigma}(t)_{\tau'} = \bar{v}_{\lambda'}(l')\Gamma' e^{m'}(q')^* u_\sigma(k_{\tau'}) \ , \end{aligned} \tag{5.7}$$

where Γ (Γ') is the coupling matrix at the unprimed (primed) vertex. We have, of course, $t=-k^2$ and $k=l-q=q'-l'$.

Let us apply these general results to the t-channel diagram for $e^-e^+\to W^-W^+$ (neutrino exchange). The general amplitude is of the structure given in Eq. (5.6). We let $M=M'=M_W$. The nonvanishing transverse vertex amplitudes are

$$\begin{aligned} j^{L\,+}_L(t)^{\tau=-} = j^-_{RL}(t)_{\tau'=+} &= 2\sqrt{-l\cdot k_-} \\ &= [2(-t+M_W{}^2)]^{1/2} \ , \end{aligned} \tag{5.8}$$

and the nonvanishing longitudinal vertex amplitudes are

$$\begin{aligned} j^{L\,0}_L(t)^{\tau=+} &= j^0_{RL}(t)_{\tau'=-} \\ &= -2[(q\cdot l)(q\cdot k_+)/q^2]^{1/2} \\ &= -[-t(-t+M_W{}^2)]^{1/2}/M_W \\ &= -\eta_t[2(-t+M_W{}^2)]^{1/2} \ . \end{aligned} \tag{5.9}$$

Hence, the factorized helicity amplitudes are, excluding a common factor of $g^2(1-M_W{}^2/t)$,

$$\begin{aligned} &f^{+-}_{LR} = \sinh\frac{\xi}{2} \ , \\ &f^{+0}_{LR} = \eta_t\cosh\frac{\xi}{2} = -f^{0-}_{LR} \ , \\ &f^{00}_{LR} = -\eta_t{}^2\sinh\frac{\xi}{2} \ , \end{aligned} \tag{5.10}$$

where

$$\eta_t = (-t/2M_W{}^2)^{1/2} \ , \tag{5.11}$$

and all other amplitudes vanish. Note that there is one power of η_t associated with each longitudinal-polarization index.

As is the case with e-W scattering of the last section, Eq.(4.16), the leptons in this process also have definite helicities, i.e., $f_{RL}=0$ irrespective of boson polarizations. This is a direct consequence of the chiral lepton-neutrino-W-boson coupling. The simplicity of the nonvanishing amplitudes, Eq. (5.10), is also striking.

VI. W^+W^- PAIR PRODUCTION

As a nontrivial realistic application, let us consider the pair production of W bosons in e^+e^- annihilation in the standard model.[1,4–6,12] The three contributing tree diagrams are given in Fig. 10. For convenience, the particle labels and charge flow are displayed in Fig. 10(a); the momentum labels in Fig. 10(b); and the helicity labels in Fig. 10(c).

The helicity amplitudes can be written down directly

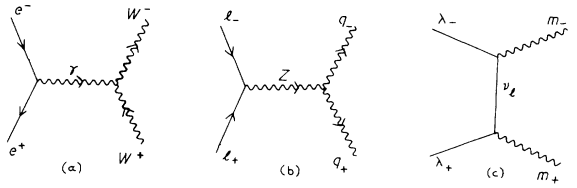

FIG. 10. Diagrams contributing to $e^-e^+ \to W^-W^+$ in the standard model.

according to the procedures outlined in preceding sections. The t-channel pole contribution [Fig. 10(c)] has already been worked out in Sec. V. From the γ^* and Z^* intermediate-state terms, Figs. 10(a) and 10(b), we obtain

$$f^{m_-m_+}_{\lambda_-\lambda_+}(s,\theta)=\frac{g_V g_f}{s-M_V{}^2}T^{m_-m_+}_m(s)d^1(-\theta)^m{}_n j^n_{\lambda_-\lambda_+}(s)\ , \tag{6.1}$$

where g_V and g_f are the three-vector-boson and the fermion-boson coupling constants, respectively. Making use of the vertex amplitudes worked out in Appendixes B and C, we obtain specifically, excluding a common factor $\sqrt{2}g_V g_f \beta s/(s-M_V{}^2)$,

$$\begin{aligned}
&f^{++}_{LR}=f^{--}_{LR}=f^{++}_{RL}=f^{--}_{RL}=d^0_\theta\ ,\\
&f^{0+}_{LR}=-f^{-0}_{LR}=-f^{0-}_{RL}=f^{+0}_{RL}=2\gamma d^+_\theta\ ,\\
&f^{0-}_{LR}=-f^{+0}_{LR}=-f^{0+}_{RL}=f^{-0}_{RL}=2\gamma d^-_\theta\ ,\\
&f^{00}_{LR}=f^{00}_{RL}=-(1+2\gamma^2)d^0_\theta\ ,
\end{aligned} \tag{6.2}$$

and all other amplitudes vanish. Here

$$\begin{aligned}
&\beta=(1-4M_W{}^2/s)^{1/2}\ ,\\
&\gamma=\sqrt{s}\,/2M_W=(1-\beta^2)^{-1/2}\ ,\\
&d^0_\theta=d^1(\theta)^0{}_1=-d^1(\theta)^0{}_{-1}=\sin\theta/\sqrt{2}\ ,\\
&d^+_\theta=d^1(\theta)^1{}_1=d^1(\theta)^{-1}{}_{-1}=(1+\cos\theta)/2\ ,\\
&d^-_\theta=d^1(\theta)^1{}_{-1}=d^1(\theta)^{-1}{}_1=(1-\cos\theta)/2\ ,
\end{aligned} \tag{6.3}$$

and

$$\begin{aligned}
g_f&=g_L \quad \text{for } (\lambda_-\lambda_+)=(LR)\\
&=g_R \quad \text{for } (\lambda_-\lambda_+)=(RL)\ .
\end{aligned} \tag{6.4}$$

We note again the simplicity of the results given by Eq. (6.2). Not only are the angular factors obvious and explicit, but the energy-dependent coefficients are also optimally exhibited: associated with each longitudinally polarized vector meson there is one power of γ. At high energies, the $f^{00}_{\lambda_-\lambda_+}$ amplitudes are the dominant ones, as is well known.

To combine the amplitudes associated with γ^* and Z^* exchange, we note that, for the former

$$\begin{aligned}
&M_V=0,\ \ s/(s-M_V{}^2)=1\ ,\\
&g^\gamma_V g^\gamma_L=g^\gamma_V g^\gamma_R=e^2\ ,
\end{aligned} \tag{6.5}$$

and for the latter

$$\begin{aligned}
&M_V=M_Z,\ \ \frac{s}{s-M_V{}^2}=\frac{s}{s-M_Z{}^2}\ ,\\
&g^Z_V g^Z_R=-e^2\ ,\\
&g^Z_V g^Z_L=-(1-\xi_L)e^2\ ,
\end{aligned} \tag{6.6}$$

where

$$\xi_L\equiv\frac{1}{2\sin^2\theta_W}\ . \tag{6.7}$$

Hence the overall factors to be multiplied to the amplitudes of Eq. (6.2) due to the combined γ^*- and Z^*-pole terms are, for $\{f_{RL}\}$

$$\begin{aligned}
N_R&=\sqrt{2}e^2\beta\left[1-\frac{s}{s-M_Z{}^2}\right]\\
&=-\sqrt{2}e^2\beta\frac{M_Z{}^2}{s-M_Z{}^2}
\end{aligned} \tag{6.8}$$

and, for $\{f_{LR}\}$,

$$\begin{aligned}
N_L&=\sqrt{2}e^2\beta\left[1-\frac{s}{s-M_Z{}^2}(1-\xi_L)\right]\\
&=\sqrt{2}e^2\beta\frac{\xi_L s-M_Z{}^2}{s-M_Z{}^2}\\
&=\frac{g^2}{\sqrt{2}}\beta\frac{s-M_Z{}^2/\xi_L}{s-M_Z{}^2}\ ,
\end{aligned} \tag{6.9}$$

where $g=e/\sin\theta_W$ is the $SU(2)_L$ gauge coupling constant. Note that N_R has a $1/s$ asymptotic energy dependence, whereas N_L is $\propto(1)$. The latter, when combined with $|f^{00}|^2$, will yield infinitely rising cross sections unless it is canceled by other contributions.[1,4–6]

We need to combine these results with contributions from the t-channel ν-exchange diagram given in Sec. V, Eq. (5.10). We cannot simply add the helicity amplitudes because the helicity labels (m_-,m_+) on the t-channel amplitudes are not the same as those on the s-channel amplitudes of Eq. (6.2). The reason is that the specification of the helicity label for a massive particle depends on a reference momentum in addition to the momentum of the particle itself. Explicitly, the polarization vector for the W^- boson is $e^{q_+}_{m_-}(q_-)^\mu$ for the s-channel amplitudes, while it is $e^{l_-}_{m_-}(q_-)^\mu$ for the t-channel amplitudes. Here the superscripts q_+ and l_- indicate the reference momenta in question. In order to combine the s-channel and t-channel amplitudes, it is necessary to transform between the two sets of polarization vectors. This transformation is a 3-rotation in the rest frame of the particle under consideration—the "Wigner rotation." In the case of $e^-e^+\to W^-W^+$, the Wigner rotation for W^- and W^+ are both of the form $R_2(\psi)$ where

$$\tan\psi=\frac{\sin\theta}{\gamma(\beta-\cos\theta)}=\frac{2M\sqrt{-t}}{-t-M^2}\tanh\frac{\xi}{2}\ . \tag{6.10}$$

This result is derived in Appendix A. Therefore, if the t-channel amplitudes in the t-channel basis are denoted by $\tilde{f}$, then their contribution to the helicity amplitudes in the s-channel basis will be of the form

$$f_{LR}^{m_-m_+}=d^{1^\dagger}(\psi)^{m_-}{}_{n_-}d^{1^\dagger}(\psi)^{m_+}{}_{n_+}\tilde{f}_{LR}^{n_-n_+}\ . \tag{6.11}$$

Using the simple results of Eq. (5.10), excluding a common factor $g^2(1-M_W{}^2/t)$ as before, we obtain [cf. Eq. (2.7)]

$$\begin{aligned}f_{LR}^{m_-m_+}=&[d^1(-\psi)^{m_-}{}_+d^1(-\psi)^{m_+}{}_- -\eta_t{}^2d^1(-\psi)^{m_-}{}_0d^1(-\psi)^{m_+}{}_0]\sinh\frac{\xi}{2}\\&+[d^1(-\psi)^{m_-}{}_+d^1(-\psi)^{m_+}{}_0-d^1(-\psi)^{m_-}{}_0d^1(-\psi)^{m_+}{}_-]\eta_t\cosh\frac{\xi}{2}\ .\end{aligned} \tag{6.12}$$

It is straightforward, though not necessary, to write the expression on the right-hand side in terms of the s-channel variables (s,θ). The following kinematic relations are useful for this purpose:

$$\begin{aligned}\sin\psi&=\frac{1}{\gamma}\frac{\sin\theta}{1-\beta\cos\theta}\ ,\\ \cos\psi&=\frac{\beta-\cos\theta}{1-\beta\cos\theta}\ ,\\ \eta_t{}^2&=\frac{-t}{2M_W{}^2}=\frac{\gamma^2}{2}(1-2\beta\cos\theta+\beta^2)\\&=\tfrac{1}{2}[2\gamma^2(1-\beta\cos\theta)-1]\ ,\\ \sinh\xi/2&=\beta\frac{\sin\theta}{1-\beta\cos\theta}=\beta\gamma\sin\psi\ ,\\ \cosh\xi/2&=\frac{\sqrt{2}}{\gamma}\frac{\eta_t}{1-\beta\cos\theta}\\&=\frac{(1-2\beta\cos\theta+\beta^2)^{1/2}}{1-\beta\cos\theta}\ ,\\ \eta_t\cosh\xi/2&=\frac{\gamma}{\sqrt{2}}\frac{1-2\beta\cos\theta+\beta^2}{1-\beta\cos\theta}\ .\end{aligned} \tag{6.13}$$

After some algebra, one can show that, excluding a common factor $-g^2/\sqrt{2}$, the nonvanishing t-channel pole contributions to the helicity amplitudes in the s-channel basis are

$$\begin{aligned}f_{LR}^{++}&=f_{LR}^{--}=2d_\theta^0(\beta-\cos\theta)(-s/4t)\ ,\\ f_{LR}^{0+}&=-f_{LR}^{-0}\\&=2\gamma\,d_\theta^+[2(\beta-\cos\theta)+1-\beta^2](-s/4t)\ ,\\ f_{LR}^{0-}&=-f_{LR}^{+0}\\&=2\gamma\,d_\theta^-[2(\beta-\cos\theta)-1+\beta^2](-s/4t)\ ,\\ f_{LR}^{00}&=-2\gamma^2d_\theta^0[2(\beta-\cos\theta)+\beta(1-\beta^2)](-s/4t)\ ,\\ f_{LR}^{-+}&=2d_\theta^0(1+\cos\theta)(-s/4t)\ ,\\ f_{LR}^{+-}&=-2d_\theta^0(1-\cos\theta)(-s/4t)\ ,\end{aligned} \tag{6.14}$$

where

$$-\frac{s}{4t}=\frac{1}{1-2\beta\cos\theta+\beta^2}\ , \tag{6.15}$$

and the d_θ functions are given in Eq. (6.3).

The results in Eq. (6.14) are presented in a form easy to compare with those of Eq. (6.2). Note, in particular, that the factors following the d_θ functions in the first four equations of Eq. (6.14) approach unity in the ultrarelativistic limit; hence, the leading contributions from the s- and t-channel diagrams cancel in that limit. This is the well-known cancellation due to the gauge coupling of the standard model which ensures that cross sections involving longitudinally polarized vector bosons satisfy unitarity. This cancellation between the s- and t-channel tree diagrams takes place not only for the leading amplitude f^{00}, but is also in effect for the subleading amplitudes $f^{0\pm}$, and even $f^{\pm\pm}$. The unitary bound on the cross sections does not require that cancellation takes place for all these subleading amplitudes.[1]

VII. APPLICATIONS TO ANGULAR CORRELATIONS

The amplitude analysis described in the preceding sections is ideally suited for use in the study of angular correlations in electroweak processes. We shall consider some general features of this type of applications here. Detailed analysis of physically interesting processes will be given in subsequent papers.[15]

Consider the production of a vector boson and its ensuing decay into a pair of fermions

$$\begin{aligned}A+B&\to V+X\\&\quad\big\lfloor\!\!\to l_1+l_2\ .\end{aligned} \tag{7.1}$$

The amplitude for the production process will be written as $f^m(s,\theta)$ where m refers to the vector-boson helicity index, and the other polarization labels are suppressed. The method of the preceding sections allows us to write down directly the factorized form of $f^m(s,\theta)$ where the dependence on the production angle θ is explicitly displayed. We now focus on the decay distribution of the (l_1l_2) pair and the resulting angular correlations.

We can apply the preceding considerations to the overall processes (cf. Fig. 11) and write the full amplitude for the process [cf. Eq. (7.1)] in the factorized form

$$f^{\lambda_1\lambda_2}=j_n^{\lambda_1\lambda_2}(M^2)^*D^1(\psi,\phi)^\dagger{}_{nm}f^m(s,\theta)\ , \tag{7.2}$$

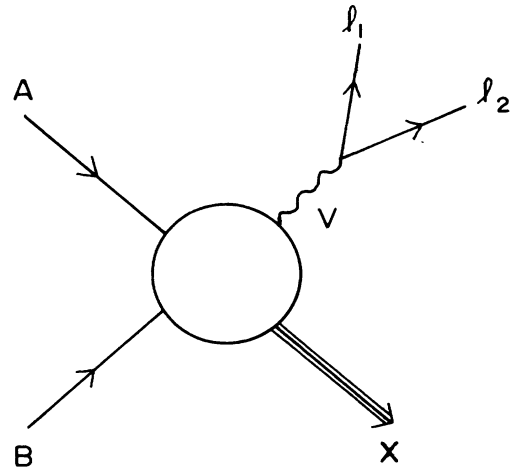

FIG. 11. Production and decay of the one-vector boson.

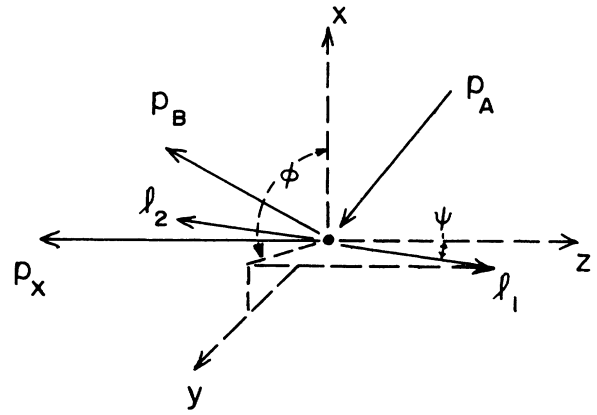

FIG. 12. Kinematics of process (7.1) in the rest frame of the vector boson, and the definition of decay angles ψ and ϕ. The z axis is opposite to p_X, the z-x plane is defined to be the primary scattering plane (spanned by p_A, p_B, and p_X).

where (ψ,ϕ) are decay angles of the $(l_1 l_2)$ pair in the rest frame of the vector boson V (with the x-z plane and the z axis determined by the production process), $D^1(\psi,\phi)^\dagger$ is the Hermitian conjugate of the spin-1 rotation matrix, and $j_n^{\lambda\lambda}$ is the decay vertex function (obtainable from Appendix B) which reduces to a constant for an on-shell V particle (see Fig. 12). We see that as the tree diagram grows the helicity amplitudes simply acquire additional factors pertaining to the extra branches. An important point is that the added factors are the same basic building blocks—the D functions and vertex amplitudes—which are characteristic of the theory.

Since the polarizations of the decay products are usually not observed, let us examine the squared matrix element summed over spins:

$$|f|^2 \equiv f^{\lambda_1\lambda_2} f^*_{\lambda_1\lambda_2} = [f^m(s,\theta) f^*_{m'}(s,\theta)] \times [j_n^{\lambda_1\lambda_2}(M^2)^* j^{n'}_{\lambda_1\lambda_2}(M^2)] \times [D^1(\psi,\phi)^{\dagger n}{}_m D^1(\psi,\phi)^{m'}{}_{n'}] \,. \tag{7.3}$$

The results of Appendix B imply a very simple structure for the factor consisting of decay amplitudes. Angular-momentum conservation requires

$$n = \lambda_1 - \lambda_2 = n' \,. \tag{7.4}$$

Moreover, we can use the chiral properties of massless fermions to determine that $n = n' = \pm 1 =$ the chirality of the fermion-boson coupling (cf. Appendix B). Thus, for the W boson of the standard model,

$$j_n^{\lambda_1\lambda_2}(M^2)^* j^{n'}_{\lambda_1\lambda_2}(M^2) = g^2 M^2 \delta_{n,-1}\delta_{n',-1} \tag{7.5}$$

and

$$|f|^2 = g^2 M^2 \Gamma(s,\theta)^m{}_{m'} \Omega(\psi,\phi)^{m'}{}_m \,, \tag{7.6}$$

where

$$\Gamma(s,\theta)^m{}_{m'} = f^m(s,\theta) f^*_{m'}(s,\theta) \,, \tag{7.7}$$

$$\Omega(\psi,\phi)^{m'}{}_m = D^1(\psi,\phi)^{m'}{}_{-1} D^{1\dagger}(\psi,\phi)^{-1}{}_m = \begin{bmatrix} s_\psi{}^4 & -\sqrt{2} s_\psi{}^3 c_\psi e^{i\phi} & s_\psi{}^2 c_\psi{}^2 e^{2i\phi} \\ -\sqrt{2} s_\psi{}^3 c_\psi e^{-i\phi} & 2 s_\psi{}^2 c_\psi{}^2 & -\sqrt{2} s_\psi c_\psi{}^3 e^{i\phi} \\ s_\psi{}^2 c_\psi{}^2 e^{-2i\phi} & -\sqrt{2} s_\psi c_\psi{}^3 e^{-i\phi} & c_\psi{}^4 \end{bmatrix} , \tag{7.8}$$

and

$$s_\psi = \sin\frac{\psi}{2} = [(1-\cos\psi)/2]^{1/2} \,, \qquad c_\psi = \cos\frac{\psi}{2} = [(1+\cos\psi)/2]^{1/2} \,. \tag{7.9}$$

Explicitly, we obtain

$$2|f|^2(g^2M^2)^{-1}=(1-\cos\psi)^2\Gamma_+^+ +2\sin^2\psi\Gamma_0^0+(1+\cos\psi)^2\Gamma_-^-$$
$$-2\sqrt{2}\sin\psi(1-\cos\psi)(\cos\phi\,\mathrm{Re}\Gamma_0^+ +\sin\phi\,\mathrm{Im}\Gamma_0^+)$$
$$-2\sqrt{2}\sin\psi(1+\cos\psi)(\cos\phi\,\mathrm{Re}\Gamma_-^0 +\sin\phi\,\mathrm{Im}\Gamma_-^0)$$
$$+2\sin^2\psi(\cos2\phi\,\mathrm{Re}\Gamma_-^+ +\sin2\phi\,\mathrm{Im}\Gamma_-^+)\ . \tag{7.10}$$

The ϕ dependence characterizes the correlation of the production and decay planes of the vector boson. The angular coefficients can be measured in a global fit to the ϕ distribution or they can be extracted individually by weighted integrals over the observed distribution with orthonormal weight functions: $\frac{1}{2}\pi^{-1}$, $\pi^{-1}\cos\phi$, $\pi^{-1}\sin\phi$, ... Likewise, the ψ distribution—either for fixed values of the other variables, or for integrated quantities over appropriate ranges and weight functions—can be analyzed to determine the coefficient functions $\Gamma(s,\theta)^m_{m'}$.

The utility of this procedure in these types of applications lies in the direct way that the theoretical expressions of $\Gamma^m_{m'}$ can be written down for any electroweak theory, and in the conveniently factorized form in which $\Gamma^m_{m'}$ themselves naturally appear as functions of the production angle θ, as well as decay angles of other final-state particles. Thus, a seemingly complex angular-correlation problem can be automatically reduced to a series of simple problems which can be analyzed iteratively. In this formalism, it is straightforward to focus on specific features of the general correlation problem which may have particular theoretical interest in testing the standard model or in the search for new physics. This method will be applied in a detailed analysis of the $e^-e^+\to W^-W^+$ process, among others, in subsequent papers.

VIII. SUMMARY

We have formulated a systematic procedure to write down helicity amplitudes for tree diagrams based on factorizing the propagators in terms of helicity four-vectors or spinors. Thus, all such amplitudes appear as products of standardized vertex amplitudes and "D functions" which express the correlation of the vertices connected by the propagators. The advantages of this approach over traditional methods can be surmised from the examples given in Secs. II—VI. We highlight some of the salient features.

(i) The basic building blocks of this formalism—the vertex amplitudes and the D functions—are both *physical*; hence, their simple structures and symmetry relations are easy to understand.

(ii) Tree diagrams for complex processes grow out of simpler tree diagrams for reduced processes. With this method, the amplitudes for the former are obtained from the latter by tagging on additional standard factors; no extra or repeated calculation is involved.

(iii) Each D-function factor contains all the dependence on the angular variables which relates to a given production or decay subprocess. Thus, this formalism is particularly suited for the analysis of angular correlations. (When more than one diagram contributes to a given process involving massive particles, an additional step involving a Wigner rotation is required, cf. Sec. VI.)

(iv) The vertex amplitudes depend only on "energy variables" (i.e., s, t, . . .). An important feature of the helicity vertex amplitudes is that they are naturally categorized according to distinct orders of magnitudes in either the high- or low-energy limits. For instance, the vanishing of the fermion-boson vertex amplitudes $\{j_\lambda^{-\lambda}\}$ reflects the fact that they are proportional to the lepton mass (which we neglect), in contrast with $\{j_\lambda^{\lambda}\}$ which are proportional to $\sqrt{s}$ [cf. Eq. (2.13)]. For the boson self-coupling vertices (where masses are not neglected), Eq. (C5) reveals the same result, as Q_1, Q_2, and Q_3 are of distinct orders of magnitudes depending on the process. This feature, together with angular-momentum conservation and other symmetry requirements, bring about very significant simplifications to the amplitudes.

The conventional method of taking traces of Dirac and Lorentz matrices, in contrast with the above, involve the following.

(i) Calculating the squares of amplitudes. This approach involves at least twice the effort of calculating the amplitudes alone. It goes in the opposite direction to the above method of factorizing the amplitudes into more basic building blocks.

(ii) Forgoing all physical information (and hence, insight) about the polarization of intermediate particles in the process. This information comes out simply in the factorized helicity-amplitude approach (cf. Secs. II—VI).

(iii) Results are expressed in terms of scalar products of four-vectors which are Lorentz invariant, but are only indirectly related to the physical energy and angular variables; hence, for complex processes, much additional work is required to exhibit the angular correlations that we discussed in the preceding section.

This amplitude analysis, emphasizing factorization, complements recent works on QCD tree-diagram calculations which utilize a spinor decomposition of massless vector-boson polarization vectors.[9–11] Since we are interested in massive vector bosons, their method does not immediately apply here. However, given timelike momentum q^μ, it can always be written as the sum of two lightlike vectors. (We used this decomposition in our treatment of the fermion propagator in Secs. IV and V.) Thus, polarization vectors of a massive vector boson can be written in terms of spinors for lightlike momenta. The connections between these two approaches, as well as the

application of this method to massless vector bosons in QED and QCD processes are currently being studied.

ACKNOWLEDGMENTS

We would like to thank J. C. Collins, L. Durand, M. Ebel, J. Gunion, Y. Kitazawa, and S. Parke for helpful discussions, and M. Aivazis for assistance in the preparation of the manuscript. This work was supported in part by the National Science Foundation Grant No. PHY-85-07635, and by the U.S. Department of Energy under Contract No. DE-FG02-85ER-40235.

APPENDIX A: CONVENTIONS AND KINEMATICS

For calculations of angular correlations, consistent phase conventions are important. It is therefore desirable to spell out our conventions explicitly.

1. Polarization indices on single-particle states

We use the Lorentz metric $(-1,1,1,1)$. In the center-of-mass (c.m.) frame of a given process, we parametrize the four-momentum of a particle by

$$p^\mu:\ (p^0,\mathbf{p})=(p^0,p\sin\theta\cos\phi,p\sin\theta\sin\phi,p\cos\theta)\ . \quad \text{(A1)}$$

The three-vector $\mathbf{p}$ is characterized by its magnitude p and the SO(3) rotation angular variables (θ,ϕ). The *helicity states* are defined by[16,17]

$$|\,\mathbf{p},\lambda\rangle\equiv R_3(\phi)R_2(\theta)\,|\,p\hat{\mathbf{z}},\lambda\rangle\ , \quad \text{(A2)}$$

where $\hat{\mathbf{z}}$ is the coordinate unit vector along the z axis, $|\,p\hat{\mathbf{z}},\lambda\rangle$ is an eigenstate of P_3 and J_3 with eigenvalues p and λ, respectively, and $\{R_i,i=1,2,3\}$ are the usual rotation operators around the ith axis.

Alternatively, in the brick-wall (BW) frame of a given process, we parametrize the four-momentum of a particle as

$$p^\mu:\ (\bar{\mathbf{p}},p^3)=(p'\cosh\xi,p'\sinh\xi\cos\phi,p'\sinh\xi\sin\phi,p^3)\ , \quad \text{(A3)}$$

where $\bar{\mathbf{p}}$ is a three-vector in the (0-1-2) space characterized by its magnitude p' and SO(2,1) "angular" variables (ξ,ϕ). The single-particle state with polarization index σ is defined as

$$|\,\bar{\mathbf{p}},\sigma\rangle=R_3(\phi)B_1(\xi)\,|\,p^3\hat{\mathbf{z}},\sigma\rangle\ , \quad \text{(A4)}$$

where B_1 is a Lorentz boost along the x axis and the state on the right-hand side is again an eigenstate of P_3 and J_3 with eigenvalues p^3 and σ, respectively. Note that p^3 can be either positive or negative. States with $p^3<0$ will be defined in terms of those with $p^3>0$ by

$$|\,-p^3\hat{\mathbf{z}},\sigma\rangle=R_2(\pi)\,|\,p^3\hat{\mathbf{z}},\sigma\rangle\ \ (p^3>0)\ , \quad \text{(A5)}$$

followed by a SO(2,1) transformation as in Eq. (A4).

2. Polarization vectors for vector bosons

Let the vector-boson momentum be q^μ. To define the polarization vectors, we need a second reference four-vector denoted by k^μ to specify the direction of quantization. If q^μ is timelike, k^μ will be spacelike, and vice versa. (If q^μ is lightlike, then the quantization axis is always along the direction of motion. One still needs a second vector to fix the gauge of the polarization vector. We shall not explicitly consider massless vector bosons in this paper.) It suffices to define all vectors in a frame where the t-z plane is spanned by (q^μ,k^μ). Other configurations are obtained by applying an appropriate Lorentz transformation to all the relevant vectors [cf. Eqs. (A2) and (A4)].

The unit four-vector proportional to q^μ will be called the *scalar polarization* vector and denoted by e_q:

$$e_q(q)^\mu:\ (q_0,0,0,q)\,|\,{q_0}^2-q^2\,|^{-1/2}\ , \quad \text{(A6)}$$

where q is the magnitude of the three-momentum. Correspondingly, the *longitudinal-polarization* vector $e_{m=0}$, is proportional to $k^\mu-q^\mu(q\cdot k)/q^2$ and can be written (in the same frame) as

$$e_0(q)^\mu:\ (q,0,0,q_0)\,|\,{q_0}^2-q^2\,|^{-1/2}\ . \quad \text{(A7)}$$

It is understood, of course, that these vectors are only relevant when q^μ is timelike or spacelike. There is no scalar or longitudinal polarization for lightlike q^μ.

For the *transverse-polarized* states, we use the *helicity* indices $\pm$ as a shorthand for $m=\pm1$, and define $e_\pm$ according to the Condon-Shortley convention:

$$e_\pm(q)^\mu:\ (0,\mp1,-i,0)/\sqrt{2}\ . \quad \text{(A8)}$$

The above specification is restricted to $q^3=q\geq0$. In applying Eq. (A4), we also need a convention for the case $q^3=-q<0$. In accordance with Eq. (A5), we obtain all relevant four-vectors in the latter case by applying the rotation $R_2(\pi)$ to the corresponding ones defined above. The explicit results are

$$\begin{aligned} &e_q(q)^\mu:\ (q_0,0,0,-q)\,|\,{q_0}^2-q^2\,|^{-1/2}\ ,\\ &e_0(q)^\mu:\ (q,0,0,-q_0)\,|\,{q_0}^2-q^2\,|^{-1/2},\ \ q^3<0\ ,\\ &e_\pm(q)^\mu:\ (0,\pm1,-i,0)/\sqrt{2}\ . \end{aligned} \quad \text{(A9)}$$

When it is desirable to make explicitly the dependence of the above definitions on the reference vector k^μ, we shall use the notation $e_m(q)^\mu=e_m^k(q)^\mu$, with $m=q,0,\pm$.

When q^μ is timelike, it is possible to go to the c.m. frame defined by $q=0$. The effect of a rotation $R_2(\theta)$ [cf. Eq. (A2)] on the polarization vector is given by the well-known result

$$\begin{aligned} &R_3(\phi)R_2(\theta)e_q^\mu=e_q^\mu\ \ \text{(scalar component)}\ ,\\ &R_3(\phi)R_2(\theta)e_m^\mu=e_n^\mu e^{-in\phi}d^1(\theta)^n{}_m\ \ \text{(vector component)}\ , \end{aligned} \quad \text{(A10)}$$

where $m,n=1,0,-1$, and

$$d^1(\theta)=\begin{bmatrix} \frac{1+\cos\theta}{2} & \frac{-\sin\theta}{\sqrt{2}} & \frac{1-\cos\theta}{2} \\ \frac{\sin\theta}{\sqrt{2}} & \cos\theta & \frac{-\sin\theta}{\sqrt{2}} \\ \frac{1-\cos\theta}{2} & \frac{\sin\theta}{\sqrt{2}} & \frac{1+\cos\theta}{2} \end{bmatrix} . \quad \text{(A11)}$$

Similarly, when q^μ is spacelike, we can go to the frame with $q^0=0$, [q^μ: (0,0,0,q)]. The effect of a Lorentz boost $B_1(\xi)$ [cf. Eq. (A4)] on the polarization vectors is given by

$$\begin{aligned} &R_3(\phi)B_1(\xi)e_q^\mu=e_q^\mu \quad \text{(scalar components)} , \\ &R_3(\phi)B_1(\xi)e_m^\mu=e_n^\mu e^{-in\phi}\tilde{d}^{\,1}(\xi)^n{}_m \quad \text{(vector components)} , \end{aligned} \quad \text{(A12)}$$

where $m,n=1,0,-1$, and

$$\tilde{d}^{\,1}(\xi)=\begin{bmatrix} \frac{1+\cosh\xi}{2} & \frac{-\sinh\xi}{\sqrt{2}} & \frac{1-\cosh\xi}{2} \\ \frac{-\sinh\xi}{\sqrt{2}} & \cosh\xi & \frac{\sinh\xi}{\sqrt{2}} \\ \frac{1-\cosh\xi}{2} & \frac{\sinh\xi}{\sqrt{2}} & \frac{1+\cosh\xi}{2} \end{bmatrix} . \quad \text{(A13)}$$

3. Helicity spinors for fermions

Since we take all external fermions to be massless, it is convenient to use the light-cone representation for the Dirac spinors and matrices. We also introduce the terminology *right- and left-moving particles* where right moving (left moving) describes a particle moving in the positive (negative) z direction.

In this representation, the spinors for a right-moving particle [p^μ: (p,0,0,p)] have only upper components:

$$u_\lambda(+)\equiv u(p\hat{\mathbf{z}},\lambda)=\sqrt{2p}\begin{bmatrix}\chi_\lambda\\0\end{bmatrix} , \quad \text{(A14)}$$

where χ_λ is Pauli 2-spinor. Explicit expressions for some of the important Dirac matrices in this representation are

$$\begin{aligned} &\alpha^3=\begin{bmatrix}1&0\\0&-1\end{bmatrix}=\gamma^0\gamma^3,\ \gamma^0=\begin{bmatrix}0&1\\1&0\end{bmatrix} , \\ &\gamma^5=\begin{bmatrix}\sigma_3&0\\0&-\sigma_3\end{bmatrix},\ \gamma^3=\begin{bmatrix}0&-1\\1&0\end{bmatrix} , \\ &\gamma^1=\begin{bmatrix}-i\sigma_2&0\\0&i\sigma_2\end{bmatrix},\ \alpha^1=\begin{bmatrix}0&i\sigma_2\\-i\sigma_2&0\end{bmatrix} , \\ &\gamma^2=\begin{bmatrix}i\sigma_1&0\\0&-i\sigma_1\end{bmatrix},\ C=\begin{bmatrix}0&\sigma_1\\-\sigma_1&0\end{bmatrix}=i\alpha^2 , \\ &\Sigma^3=\begin{bmatrix}\sigma_3&0\\0&\sigma_3\end{bmatrix}=i\gamma^1\gamma^2,\ \Sigma^{1,2}=\begin{bmatrix}0&\sigma_{1,2}\\\sigma_{1,2}&0\end{bmatrix} . \end{aligned} \quad \text{(A15)}$$

Since the rotation $R_2(\pi)$ flips upper and lower components,

$$\begin{aligned} u_\lambda(-)\equiv u(-p\hat{\mathbf{z}},\lambda)&\equiv R_2(\pi)u_\lambda(+) \\ &=-i\Sigma_2 u_\lambda(+) \\ &=(2\lambda)\sqrt{2p}\begin{bmatrix}0\\\chi_{-\lambda}\end{bmatrix} , \end{aligned} \quad \text{(A16)}$$

where $\Sigma_2=i\gamma^3\gamma^1$ is twice the generator of R_2. Thus, the u spinor for a left-moving particle has only lower components.

The spin for an antifermion is related to the corresponding one for a fermion by

$$v^\lambda(\pm)\equiv C\bar{u}^{\,\lambda}(\pm)^T=C\gamma^{0T}u_\lambda(\pm)^*=u_{-\lambda}(\pm) . \quad \text{(A17)}$$

This feature (for massless fermions only) leads to many simplifications in practical calculations using the light-cone representation.

The spinors for particles moving in an arbitrary direction are obtained from $u_\lambda(\pm)$ by a rotation $R_2(\theta)$ [cf. Eq. (A2)] or a boost $B_1(\xi)$ [cf. Eq. (A4)] followed by $R_3(\phi)$, if necessary. For our own applications ($\phi=0$), it is useful to express the general spinors as linear combinations of the standard spinors defined above. We obtain

$$\begin{aligned} u_\lambda^\theta(\pm)&\equiv R_2(\theta)u_\lambda(\pm) \\ &=\left[\cos\frac{\theta}{2}-i\Sigma_2\sin\frac{\theta}{2}\right]u_\lambda(\pm) . \end{aligned} \quad \text{(A18)}$$

According to Eq. (A16), we have

$$-i\Sigma_2 u_\lambda(\pm)=\pm u_\lambda(\mp) ; \quad \text{(A19)}$$

hence,

$$u_\lambda^\theta(\pm)=\cos\frac{\theta}{2}u_\lambda(\pm)\pm\sin\frac{\theta}{2}u_\lambda(\mp) . \quad \text{(A20)}$$

In other words,

$$u_\lambda^\theta(\tau)\equiv R_2(\theta)u_\lambda(\tau)=u_\lambda(\tau')d^{1/2}(\theta)^{\tau'}{}_\tau , \quad \text{(A21)}$$

where $\tau,\tau'=\pm$ and $d^{1/2}(\theta)$ is the familiar rotation matrix:

$$d^{1/2}(\theta)=\begin{bmatrix}\cos\frac{\theta}{2}&-\sin\frac{\theta}{2}\\\sin\frac{\theta}{2}&\cos\frac{\theta}{2}\end{bmatrix} . \quad \text{(A22)}$$

Note that the helicity index λ stays invariant under a rotation, as expected for massless particles. Since, under a rotation, the $\pm z$ directions become mixed, the rotation matrix $d^{1/2}(\theta)$ acts on the $\tau=\pm$ index of the spinors $u_\lambda(\tau)$ instead. This is an understandable, but not altogether familiar, result.

In the brick-wall frame we also encounter

$$u_\lambda^\xi(\pm)\equiv B_1(\xi)u_\lambda(\pm)=\left[\cosh\frac{\xi}{2}+\alpha_1\sinh\frac{\xi}{2}\right]u_\lambda(\pm) . \quad \text{(A23)}$$

It is straightforward to see that

$$\alpha_1 u_\lambda(\pm)=\mp i\Sigma_2 u_\lambda(\pm)=u_\lambda(\mp) ; \quad \text{(A24)}$$

hence,

$$u_{\lambda}^{\xi}(\tau)=u_{\lambda}(\tau')\tilde{d}^{1/2}(\xi)^{\tau'}{}_{\tau}\ , \tag{A25}$$

where $\tilde{d}$ is the "spin-$\frac{1}{2}$" SO(2,1) rotation matrix [corresponding to Eq. (A22)],

$$\tilde{d}^{1/2}(\xi)=\begin{bmatrix}\cosh\frac{\xi}{2} & \sinh\frac{\xi}{2}\\ \sinh\frac{\xi}{2} & \cosh\frac{\xi}{2}\end{bmatrix}\ . \tag{A26}$$

The interpretation of Eq. (A25) is identical to that of Eq. (A21) [cf. discussion after Eq. (A22)].

We shall let the helicity index λ for spinors take the values R (L), i.e., right handed (left handed), for $\lambda=\frac{1}{2}$ ($-\frac{1}{2}$):

$$\begin{aligned}u_{R,L}(\tau)&=u_{\lambda=\pm1/2}(\tau)\ ,\\ v^{R,L}(\tau)&=v^{\lambda=\pm1/2}(\tau)\ .\end{aligned} \tag{A27}$$

For these massless spinors, the helicity is directly related to the chirality, as can be seen from the fact that the chirality projection matrices are

$$\Gamma_{R,L}=\tfrac{1}{2}(1\pm\gamma^5)=\tfrac{1}{2}\begin{bmatrix}1\pm\sigma_3 & 0\\ 0 & 1\mp\sigma_3\end{bmatrix}\ . \tag{A28}$$

Thus, for fermion spinors [$u_{\lambda}(\tau)$], $\Gamma_{R(L)}$ projects out the R (L) helicity; whereas, for the antifermion spinors [$v^{\lambda}(\tau)=u_{-\lambda}(\tau)$], $\Gamma_{R(L)}$ projects out the L (R) helicity. We have, specifically,

$$\begin{aligned}\Gamma_L u_R=\Gamma_L v^L=\bar{u}^L\Gamma_L=\bar{v}_R\Gamma_L=0\ ,\\ \Gamma_R u_L=\Gamma_R v^R=\bar{u}^R\Gamma_R=\bar{v}_L\Gamma_R=0\ ,\end{aligned} \tag{A29}$$

which we shall make use of frequently.

4. Wigner rotation

Wigner rotations arise when there is a change of quantization axis in the precise definition of the polarization index of a particle of *nonzero mass*. We consider the special case for the vector mesons $W^{\pm}$ in the process $e^-e^+\to W^-W^+$.

Consider the c.m. frame with the z axis along the direction of W^- (Fig. 13). The relevant vectors, in component form, are

$$\begin{aligned}q_-^{\mu}:&\ \frac{\sqrt{s}}{2}(1,0,0,\beta)\ ,\\ q_+^{\mu}:&\ \frac{\sqrt{s}}{2}(1,0,0,-\beta)\ ,\\ l_-^{\mu}:&\ \frac{\sqrt{s}}{2}(1,-\sin\theta,0,\cos\theta)\ ,\\ l_+^{\mu}:&\ \frac{\sqrt{s}}{2}(1,\sin\theta,0,-\cos\theta)\ ,\end{aligned} \tag{A30}$$

where $\beta=(1-4M^2/s)^{1/2}$ and $M=M_W$. We apply a Lorentz transformation along the negative z axis to get to the rest frame of W^- (Fig. 13). The four-vectors above become

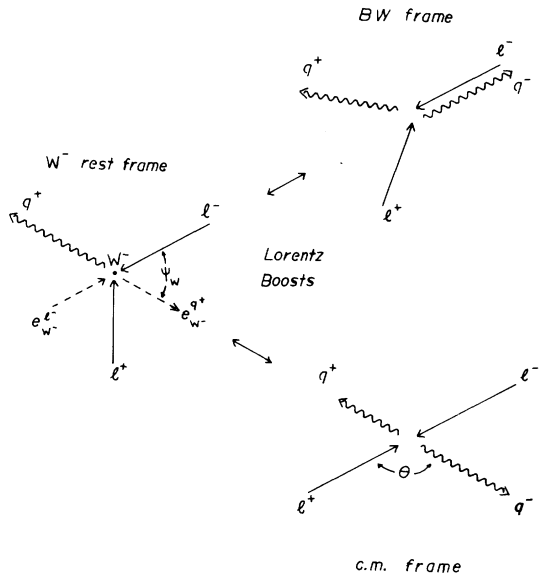

FIG. 13. Origin of the Wigner rotation. The Wigner rotation angle is denoted by ψ_W.

$$\begin{aligned}q_-^{\mu}:&\ (M,0,0,0)\ ,\\ q_+^{\mu}:&\ \left[\frac{s-2M^2}{2M},0,0,\frac{-s}{2M}\beta\right]\ ,\\ l_-^{\mu}:&\ \left[\frac{-t+M^2}{2M},\frac{-\sqrt{s}}{2}\sin\theta,0,\frac{s}{4M}(\cos\theta-\beta)\right]\ ,\\ l_+^{\mu}:&\ \left[\frac{-u+M^2}{2M},\frac{+\sqrt{s}}{2}\sin\theta,0,\frac{s}{4M}(-\cos\theta-\beta)\right]\ .\end{aligned} \tag{A31}$$

The Wigner rotation angle Ψ_W is that between the three-vectors $\mathbf{q}_+$ (which determines the "z axis" of the c.m. frame) and $\mathbf{l}_-$ (which determines the "z axis" of the BW frame). We obtain

$$\tan\Psi_W=\frac{2M}{\sqrt{s}}\frac{\sin\theta}{\beta-\cos\theta}=\frac{1}{\gamma}\frac{\sin\theta}{\beta-\cos\theta}\ , \tag{A32}$$

from which it follows that

$$\begin{aligned}\sin\Psi_W&=\frac{\sin\theta}{\gamma(1-\beta\cos\theta)}\ ,\\ \cos\Psi_W&=\frac{\beta-\cos\theta}{(1-\beta\cos\theta)}\ ,\\ 1\pm\cos\Psi_W&=\frac{(1\mp\cos\theta)(1\pm\beta)}{(1-\beta\cos\theta)}\ ,\end{aligned} \tag{A33}$$

and

$$e_m^{l-}(q_-)^{\mu}=e_n^{q+}(q_-)^{\mu}d^1(-\Psi_W)^n{}_m\ . \tag{A34}$$

It is also of interest to express Ψ_W in terms of t-channel

variables (t,ξ). This can easily be done by repeating the above derivation starting from the BW-frame configuration. The result is

$$\tan\Psi_W=\frac{2M\sqrt{-t}}{-t-M^2}\tanh\frac{\xi}{2}\ . \tag{A35}$$

Equating the right-hand side of Eqs. (A32) and (A35), we can express ξ in terms of the other variables. In particular, one can show that

$$\sinh\frac{\xi}{2}=\beta\frac{\sin\theta}{1-\beta\cos\theta}\ . \tag{A36}$$

APPENDIX B: FERMION-BOSON VERTEX AMPLITUDES

The fermion-boson vertex amplitude is of the general form

$$U^\dagger(p',\lambda')\gamma^0\not{e}^{\,m}(q)^*\Gamma_\kappa U(p,\lambda)\ , \tag{B1}$$

where U is either a u spinor (particle) or a v spinor (antiparticle), p and p' are along the z axis, m takes on the values $(+,0,-,q)$, and $\Gamma_\kappa=(1\pm\gamma^5)/2$ are the chirality projection matrices. The structure of this vertex amplitude depends on the signs of p and p', but not on their magnitudes; hence, we shall use the notation of Appendix A where $U_\lambda(\pm)=U(p\gtrless 0,\lambda)$ represent right- and left-moving fermion spinors. According to the discussions of Appendix A, $U_\lambda(+)$ [$U_\lambda(-)$] have only upper [lower] components. It is also useful to bear the following in mind.

(i) The antiparticle spinors are given by the corresponding particle ones with the opposite helicity index [Eq. (A17)]:

$$v^\lambda(\pm)=u_{-\lambda}(\pm)\ . \tag{B2}$$

(ii) The spin projection along the z direction has the following effect:

$$\begin{aligned}\Sigma^3 u_\lambda(\pm)&=(\pm 2\lambda)u_\lambda(\pm)\ ,\\ \Sigma^3 v^\lambda(\pm)&=(\mp 2\lambda)v^\lambda(\pm)\ .\end{aligned} \tag{B3}$$

(iii) We do not necessarily require that p, p', and q satisfy a momentum-conservation constraint due to the fact that one of the spinors can arise from the decomposition of a fermion propagator (cf. Sec. IV), and hence can carry an unphysical lightlike momentum.

The general vector—axial-vector vertex, Eq (B1), is *chirality conserving* because $\gamma^0\not{e}_m$ commutes with Γ_κ for all m; hence, $U(p,\lambda)$, and $U^\dagger(p',\lambda')$ must have the same chirality. This fact, together with Eq. (A29) imply the following rules.

Chirality rule. The chiralities of both fermions at the fermion-boson vertex must be the same as that of the coupling Γ_κ.

Helicity rule. If the two Dirac spinors in Eq. (B1) are a pair of u's or a pair of v's (i.e., one fermion in the initial state and the other in the final state) then the helicities are the same; if they are a mixed pair (i.e., both fermions are in the initial state or in the final state) then the helicities must be opposite [cf. Eqs. (A28), (A29), and (B3)]. In both cases, the total fermion helicity (algebraic sum) is conserved between initial and final states.

To proceed further, it is convenient to distinguish the transverse polarizations of the vector boson from the longitudinal and scalar ones.

1. Transverse-polarizations rules

For transverse-polarized right-moving bosons, the matrices $\gamma^0\not{e}^{\,\pm *}$ are of the form

$$\gamma^0\not{e}^{\,\pm *}=\sqrt{2}\begin{bmatrix}0 & \sigma_\mp\\ -\sigma_\mp & 0\end{bmatrix}\ \text{where}\ \sigma_\pm=\tfrac{1}{2}(\sigma_1\pm i\sigma_2)\ . \tag{B4}$$

They flip upper and lower components of Dirac spinors; hence, (i) transversely polarized bosons only connect fermion states moving in *opposite* directions.

It is also easy to see that when applied to right-moving lightlike spinors

$$\not{e}^{\,+*}\Gamma_L u(+)=0=\not{e}^{\,-*}\Gamma_R u(+)\ . \tag{B5}$$

In other words, (ii) for nonvanishing amplitudes, the handedness of an outgoing right-moving boson must be the same as the chirality of the coupling.

Quantitatively, we begin with the specific vertex amplitude describing the process $l\to l'+V$, obtaining

$$j_\lambda^{\lambda' m}=\bar u^{\,\lambda'}(l')\not{e}^{\,m*}\Gamma_\kappa u_\lambda(l)=(-\kappa)2\sqrt{-l\cdot l'}\ . \tag{B6}$$

This is illustrated in Fig. 14 for the case of a *left-handed coupling,* where the double-lined arrows depict spin projections, l and V are right moving and l' is left moving. This result, together with the fermion chirality rule implies that (iii) for a given type of chiral coupling, there is only *one* nonvanishing transverse helicity amplitude. The magnitude of this amplitude is $2(-p\cdot p')^{1/2}$; the sign is $-\kappa=-1(+1)$ for right- (left-) handed couplings.

To obtain the transverse vertex amplitudes for all other configurations, we need only transform the specific vertex of Fig. 14 by the following rules, all of which are easily derived from Eq. (B1) using properties of u_λ, v^λ, and e_m described previously.

(iv) *To cross a fermion line* from the initial state to the final state or vice versa (i.e., let $u\leftrightarrow v$), reverse the helicity of the particle with no other changes.

For example, by crossing the l' line of Fig. 14, we obtain the vertex amplitude for boson production as shown in Fig. 15.

(v) *To cross the boson line* (i.e., let $e^*\leftrightarrow e$), reverse the helicity of the boson and change the sign of the amplitude.

Similarly, by crossing the boson line of Fig. 14, we obtain the vertex amplitude of Fig. 16 (Ref. 18).

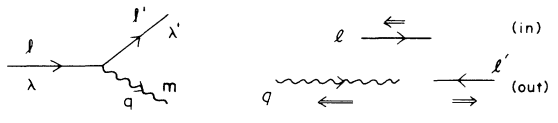

FIG. 14. Diagrammatic illustration of the vertex amplitude of Eq. (B6) for a left-handed coupling.

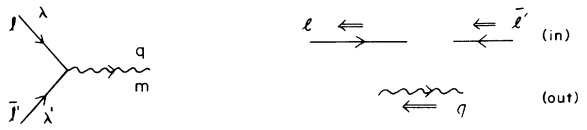

FIG. 15. Vertex amplitude obtained from Fig. 14 by crossing a fermion line.

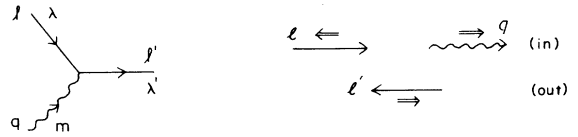

FIG. 16. Vertex amplitude obtained from Fig. 14 by crossing a boson line.

(vi) *To reverse the direction of motion of the boson,* invert the sign of its helicity with no other changes. Thus, a variation of Fig. 16 is shown in Fig. 17.

(vii) *To reverse the direction of motion of both the fermions,* reverse the helicity of the vector boson and change the sign of the amplitude.

For instance, we can apply rule (vi) to Fig. 15 to obtain the vertex amplitude of Fig. 18. The last result can be seen from Eq. (B6) by noting that complex conjugation of the amplitude brings about an interchange of $u(p)$ and $u(p')$ and thereby a reversal of the direction of motion of the fermions. Alternatively, we note

$$\begin{aligned}\bar{u}^{\lambda'}(+)\not{e}^{m*}\Gamma_\kappa u_\lambda(-)&\equiv\bar{u}^{\lambda'}(+)\not{e}^{m*}\Gamma_\kappa R_2(\pi)u_\lambda(+)\\&=-\bar{u}^{\lambda'}(+)R_2{}^{-1}(\pi)[R_2{}^{-1}(\pi)\not{e}^{m*}R_2(\pi)]\Gamma_\kappa u_\lambda(+)=\bar{u}^{\lambda'}(+)R_2^{\dagger}(\pi)\not{e}_m\Gamma_\kappa u_\lambda(+)\\&\equiv\bar{u}^{\lambda'}(-)\not{e}_m\Gamma_\kappa u_\lambda(+)\equiv-\bar{u}^{\lambda'}(-)\not{e}^{-m*}\Gamma_\kappa u_\lambda(+)\,,\end{aligned}\tag{B7}$$

where in the second step we used $R_2(2\pi)=-1$ for fermions.

2. Longitudinal and scalar polarizations

We now turn to longitudinal and scalar polarizations. The matrices $\gamma^0\not{e}_q$ and $\gamma^0\not{e}_0$ are linear compilations of the identity matrix and $\alpha_3=\left(\begin{smallmatrix}1&0\\0&-1\end{smallmatrix}\right)$. They do not flip upper and lower components; hence (i) scalar and longitudinal bosons only connect states moving in the *same* direction.

We begin with the case where the fermions are right moving and the boson is left moving. Since the amplitude is Lorentz invariant, we can evaluate it in any frame and express the results in terms of invariants. Again, we start with a specific vertex amplitude corresponding to $l+V\rightarrow l'$. For the longitudinal polarization

$$\begin{aligned}j^{\lambda}_{\lambda,0}&=\bar{u}^{\lambda}(p')\not{e}_0\Gamma_\lambda u_\lambda(p)\\&=-2[(e_q\cdot p)(e_q\cdot p')]^{1/2}\end{aligned}\tag{B8}$$

and for the scalar polarization

$$\begin{aligned}j^{\lambda}_{\lambda,q}&=\bar{u}^{\lambda}(p')\not{e}_q\Gamma_\lambda u_\lambda(p)\\&=-2[(e_q\cdot p)(e_q\cdot p')]^{1/2}\,.\end{aligned}\tag{B9}$$

The left and right chiral couplings have the same sign. This is summarized in Fig. 19 for the case of a *left chiral coupling,* where m takes on the values 0 for longitudinal and q for scalar polarizations.

As before, all nonvanishing vertex amplitudes can be obtained from this specific vertex amplitude. The rules for calculating these amplitudes in general are the following.

(ii) *To cross a fermion line,* reverse the helicity of that particle with no other changes.

(iii) *To cross a boson line,* no changes to the amplitude are necessary ($e^{0,q*}=e_{0,q}$).

(iv) *To reverse the direction of motion of a boson line* (a) for longitudinal polarization, multiply the amplitude by $-(+)$ if the boson is timelike (spacelike), (b) for scalar polarization, multiply the amplitude by $+(-)$ if the boson is timelike (spacelike).

(v) *To reverse the direction of motion of the fermions,* make the same change as in (iv).

The last result follows from the fact that

$$\bar{u}^{\lambda}(-)\not{e}_m\Gamma_\kappa u_\lambda(-)=\bar{u}^{\lambda}(+)R_2{}^{-1}(\pi)\not{e}_m R_2(\pi)\Gamma_\kappa u_\lambda(+)\,;\tag{B10}$$

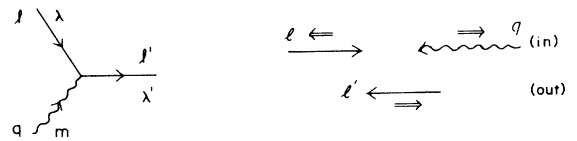

FIG. 17. Same as Fig. 16 with the direction of the boson momentum reversed.

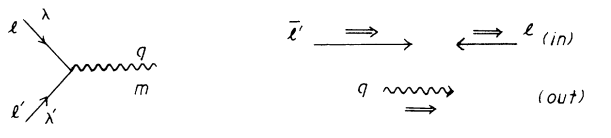

FIG. 18. Same as Fig. 15 with the directions of the fermion lines reversed.

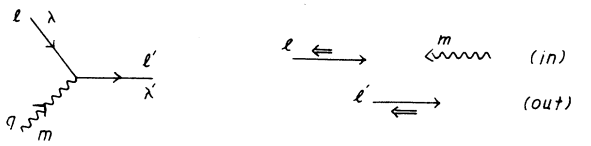

FIG. 19. Diagrammatic illustration of vertex amplitudes of Eqs. (B8) and (B9).

hence, the effect of changing the direction of the fermions is the same as changing the direction of the boson.

APPENDIX C: THREE-VECTOR-BOSON SELF-COUPLING VERTEX AMPLITUDES

The vector-boson self-coupling vertex consists of a space-time factor and a flavor matrix factor. The former is universal; the latter depends on the choice of gauge group and other specifics of the model. In this appendix we work out the standard space-time part of the vertex amplitudes.

The Lorentz tensor of the trilinear gauge coupling of three-vector bosons is given by

$$C^{\lambda\mu\nu}(k_1,k_2,k_3)=g^{\lambda\mu}(k_1-k_2)^{\nu} +g^{\mu\nu}(k_2-k_3)^{\lambda}+g^{\nu\lambda}(k_3-k_1)^{\mu} , \quad \text{(C1)}$$

where all three momenta are directed into the vertex. The momentum-conservation condition $k_1+k_2+k_3=0$ is always assumed.

We begin by examining a vertex amplitude with the following specific configuration (see Fig. 20):

$$T_I^{mn}(q_1^2,q_2^2,q_3^2)=e^m(q_2)_\mu^* e^n(q_3)_\nu^* \times C^{\lambda\mu\nu}(q_1,-q_2,-q_3)e_l(q_1)_\lambda . \quad \text{(C2)}$$

In application, at least one of the three momenta is timelike. We assume q_1^μ is timelike, but let q_2^μ and q_3^μ be unrestricted. As usual, we choose the t-z plane to coincide with that spanned by the vectors $\{q_i\}$. The vertex amplitude is invariant with respect to Lorentz boosts along the common axis. It is most easily evaluated in the c.m. frame of q_1^μ, in which

$$\begin{aligned} q_1^\mu&: (Q_1,0,0,0) , \\ q_2^\mu&: (-q_1^2-q_2^2+q_3^2,0,0,\Delta^2)/2Q_1 , \\ q_3^\mu&: (-q_1^2+q_2^2-q_3^2,0,0,-\Delta^2)/2Q_1 , \end{aligned} \quad \text{(C3)}$$

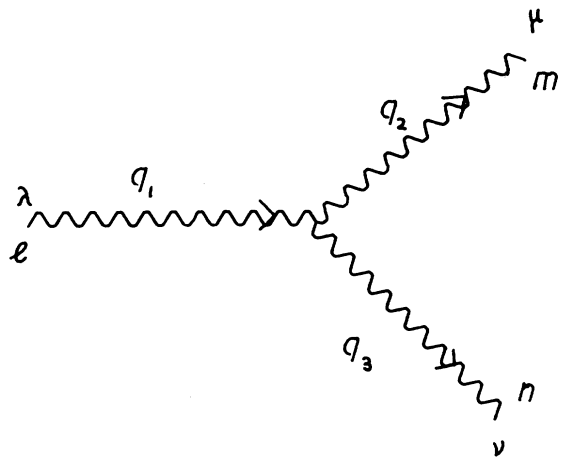

FIG. 20. The three-vector-boson vertex.

where $Q_i=|q_i^2|^{1/2}$, and the "triangle function" Δ is defined by

$$\Delta^2=(q_1^4+q_2^4+q_3^4-2q_1^2q_2^2 -2q_2^2q_3^2-2q_3^2q_1^2)^{1/2} . \quad \text{(C4)}$$

The helicity polarization vectors corresponding to these momenta are given by the rules of Appendix A.

Angular-momentum conservation, parity, and other symmetry relations reduce the 27 vertex amplitudes, Eq. (C1), to a handful. It is straightforward to verify that the only nonvanishing amplitudes are

$$\begin{aligned} T_0^{+,+}&=T_0^{-,-}=\frac{\Delta^2}{Q_1} , \\ T_+^{0,-}&=T_-^{0,+}=\frac{\Delta^2}{Q_2} , \\ T_+^{+,0}&=T_-^{-,0}=\frac{-\Delta^2}{Q_3} , \\ T_0^{0,0}&=\Delta^2(q_1^2+q_2^2+q_3^2)/2Q_1Q_2Q_3 , \end{aligned} \quad \text{(C5)}$$

where the helicity indices $\pm,0$ stand for $m=\pm1,0$.

Since the above results are presented in a manifestly symmetric form, it is clear that they also apply to the general case when no restriction is placed on the directions of the various lines. For each case, some attention is needed to obtain the correct signs for the amplitudes and the helicity indices.

[1]M. J. Duncan, G. L. Kane, and W. W. Repko, Phys. Rev. Lett. **55**, 773 (1985); Nucl. Phys. **B272**, 517 (1986).

[2]S. Dawson and J. L. Rosner, Phys. Lett. **148B**, 497 (1984); M. S. Chanowitz and M. K. Gaillard, *ibid.* **142B**, 85 (1984); P. Taxil, Centre de Physique Theorique Report No. CPT-85/P-1802, 1985 (unpublished); F. M. Renard, Laboratoire de Physique Mathematique, Montpellier Report No. PM/85-11, 1985 (unpublished).

[3]M. Hellmund and G. Ranft, Z. Phys. C **12**, 333 (1982); B. Humpert, Phys. Lett. **135**, 179 (1984).

[4]W. Alles, C. Boyer, and A. J. Buras, Nucl. Phys. **B119**, 125 (1977).

[5]F. Bletzacker and H. T. Nieh, Nucl. Phys. **B124**, 511 (1977).

[6]R. W. Brown and K. O. Mikaelian, Phys. Rev. D **19**, 922 (1979); R. W. Brown, D. Sahdev, and K. O. Mikaelian, *ibid.* **20**, 1164 (1979); R. W. Brown, K. L. Kowalski, and S. J. Brodsky, *ibid.* **28**, 624 (1983); C. L. Bilchak, R. W. Brown, and J. D. Stroughair, *ibid.* **29**, 375 (1984); J. D. Stroughair

and C. L. Bilchak, Z. Phys. C **23**, 377 (1984); C. L. Bilchak and J. D. Stroughair, Phys. Rev. D **30**, 1881 (1984); J. D. Stroughair and C. L. Bilchak, Z. Phys. C **26**, 415 (1984); J. Maalampi, D. Schildknecht, and K. H. Schwarzer, Phys. Lett. **166B**, 361 (1986).

[7]P. Mery and M. Perrottet, Nucl. Phys. **B175**, 234 (1980); D. A. Dicus and K. Kallianpur, Phys. Rev. D **32**, 35 (1985); P. Kalyniak, J. N. Ng, and P. Zakarauskas, *ibid.* **29**, 502 (1984).

[8]K.-I. Hikasa, Phys. Rev. D **33**, 3203 (1986); K. Hagiwara and D. Zeppenfeld, Nucl. Phys. **B274**, 1 (1986); K. Hagiwara, R. D. Peccei, D. Zeppenfeld, and K. Hikasa, Madison Report No. MAD/PH/279, 1986 (unpublished).

[9]P. De Causmaecker, R. Gastmans, W. Troost, and T. T. Wu, Nucl. Phys. **B206**, 53 (1982); F. A. Berends, R. Kleiss, P. De Causmaecker, R. Gastmans, W. Troost, and T. T. Wu, *ibid.* **B206**, 61 (1982).

[10]Z. Xu, D.-H. Zhang, and L. Chang, Tsinghua University Report No. TUTP-84/3, 1984 (unpublished); Tsinghua University Report No. TUTP-84/4, 1985 (unpublished); Tsinghua University Report No. TUTP-84/5, 1985 (unpublished).

[11]J. F. Gunion and Z. Kunszt, Phys. Lett. **159B**, 167 (1985); **161B**, 333 (1985); Phys. Rev. D **33**, 665 (1986).

[12]K. J. F. Gaemers and G. L. Gounaris, Z. Phys. C **1**, 259 (1979); R. Philippe, Phys. Rev. D **26**, 1588 (1982).

[13]T. P. Cheng and W.-K. Tung, Phys. Rev. D **3**, 733 (1971); P. H. Frampton and W.-K. Tung, *ibid.* **3**, 1114 (1971).

[14]M. Toller, Nuovo Cimento **A37**, 631 (1965).

[15]F. Olness and W.-K. Tung, Phys. Lett. **179B**, 269 (1985).

[16]M. Jacob and G. C. Wick, Ann. Phys. (N.Y.) **7**, 404 (1959).

[17]W.-K. Tung, *Group Theory in Physics* (World Scientific, Singapore, 1985).

[18]In case the reader may be bothered by the apparent lack of conservation of momentum here, please see remark (iii) below Eq. (B3).